Nano-confined water within the membrane of self-assembled vesicles

by

Audren Marquez

A thesis
presented to the University of Waterloo
in fulfillment of the
thesis requirement for the degree of

Master of Science

in

Chemistry

Waterloo, Ontario, Canada, 2021

Author's Declaration

I hereby declare that I am the sole author of this thesis. This is a true copy of the thesis, including any required final revisions, as accepted by the examiners.

I understand that my thesis may be made electronically available to the public.

Abstract

The hydrophobic metal carbonyl complexes, known as FpR (Fp = (Cp)Fe(PPh_3)(CO)(CO−), Cp = cyclopentadiene, R = C_3Bithiophene, C_6Pyrene, C_6Azobenzene or C_6), self-assembles into stable colloids in water. The colloids are known as metal carbonyl vesicles (MCsome), whose membrane contains interstitial water within tetrahedral order in hydrogen bonds. This well-structured water is responsible for the structural integrity of MCsome. This role of interstitial water is influenced by a variety of factors, including aging the MCsome, the non-polar R-group within the membrane and the presence of a water miscible organic solvent. In this thesis, we first examined how the colloid preparation (addition of water to THF solution of FpR) is sensitive to the quality of water used, the order of mixing water and THF solution of FpR and the rate of water addition. Following the colloidal preparation, we investigated the effect of temperature on MCsome. A higher temperature induces the swelling of MCsome, while cooling to a lower temperature shrinks the MCsome. This behaviour is found to be related to the interstitial water as its polarity and cohesive energy is affected the temperature. With higher temperatures, the polarity increases and the cohesive energy decreases, while cooling to a lower temperature decreases polarity and increases cohesive energy. This behaviour is explained by the temperature-dependent change in the interstitial water structure and dynamics. The change in the interstitial water structure and dynamics influences the energy dissipation as indicated by the temperature-dependent fluorescence intensity of FpC_6Pyrene where increasing temperature decreases the energy dissipation of the interstitial water. Using the knowledge obtained from the investigation, it was found that the cooling temperature of the colloids is important in the reconstruction of the interstitial water. Colder temperatures are found to restructure the interstitial water more quickly unlike cooling to room temperature. Furthermore, the changes in the temperature-dependent interstitial water are reversible when the temperature is below 40 °C since the restructure of the interstitial water is quick. Therefore, FpR MCsome is an ideal assembly model for the study of interstitial water confined with self-assembled nano-spaces, which is highly desirable knowledge for the design of novel colloids and understanding biological systems.

Acknowledgements

I would like to thank Dr. Xiaosong Wang for accepting me into his research lab and for providing me the constant help and support needed throughout this project.

I would also like to thank every member of the Wang group who has assisted and supported me tremendously during my time in the lab. I would like to thank Yang Yang for teaching me the experiments and knowledge needed for this project, Snehasish Modal for his insightful discussion on the project and experiments, and for creating a great lab environment, Rebecca Lo for also creating an amazing lab/office environment and for helping me throughout my time in the lab, Anni Pan for her insightful discussion about the projects, and Joshua Marquez for his help on the experiments.

Finally, I would like to thank my loving family for always being there throughout my time as a Master student. I would have not been in the position that I am in right now without their continued love and support.

Table of Contents

List of Figures

List of Tables

List of Abbreviations

AFM	Atomic force microscopy
AOT	Aerosol-OT
BT	Bithiophene
C_0	Concentration of surfactant
CMC	Critical micelle concentration
C_n	C_nH_{2n}
CNTs	Carbon nanotubes
C_{pp}	Critical packing parameter
Cryo-TEM	Cryogenic transmission electron microscopy
CV	Cyclic voltammetry
CWC	Critical water content
D_h	Hydrodynamic diameter
DLS	Dynamic light scattering
Fp	$(PPh_3)(Cp)Fe(CO)(CO-)$
FTIR	Fourier transform infrared spectroscopy
HAMAND	Hypothetical addition multivariate analysis with numerical differentiation
MCsomes	Metal carbonyl vesicles
n_w	Average coordination number of water molecules
PDI	Polydispersity index

PFS	Poly(ferrocenylsilane)
R-group	C_6, C_6Pyrene, C_6Azobenzene, or C_3Bithiophene
R_g	Radius of gyration
R_h	Hydrodynamic radius
SAXS	Small angle X-ray scattering
SC	Solute correlated
SLS	Static light scattering
TcAChE	*Torpedo californica* acetylcholinesterase
THF	Tetrahydrofuran
v%	Volume ratio
w_0	Number of water molecules per surfactant molecule
WCI	Water carbonyl interaction
$\Delta E_{1/2}$	Voltammetric peak separation
λ	Hydration level
ζ	Zeta potential

1. Introduction

1.1 Surfactants self-assembly

Self-assembly is a process, in which molecules assemble themselves into stable structures *via* molecular interactions. Surfactant molecules are the most common type of self-assembling building blocks,[1] which are surface active and contain two main components: hydrophilic polar group and hydrophobic non-polar group.[1,2] The hydrophilic group can be classified into 4 groups: anionic, cationic, zwitterionic, and non-ionic.[2] Anionic surfactants consist of hydrophilic anionic functional groups such as sulfonate and phosphate groups, such as phospholipids in biological molecules and carboxylate salts commonly used in soaps.[2] Cationic surfactants contain positively charged such as amines.[2] Zwitterionic surfactants contain both anionic and cationic groups.[2] Non-ionic surfactants contains water-soluble neutral segment, such as oxygen-containing groups that are soluble in water due to the hydrogen bonding between the oxygen-containing group and water.[2] The hydrophobic group normally contains a long hydrocarbon chain that can be saturated or unsaturated.[2]

In bulk water, a critical concentration is needed for the self-assembly of surfactants to occur, which is known as the critical micelle concentration (CMC).[3] If the concentration of the surfactant (C_0) is lower than the CMC, a layer of surfactant forms on the surface where the hydrophilic group is submerged in the water while the hydrophobic group extends out into the air or hydrophobic phase.[2,3] When the C_0 reaches the CMC, the surfactants self-assemble themselves into aggregates such as micelles.[3] The morphology of these assemblies is determined by the critical packing parameter (C_{pp}), where the molecular geometry of the surfactant molecules and the solution conditions determine this parameter.[2]

The self-assembly process of these surfactant molecules occurs due to a relevant number of what are called “soft-interactions”.[2] These soft interactions combined can strongly hold these surfactant molecules together to form stable assemblies in solution.[2] The two main interactions that are in play in the self-assembly of surfactant molecules are hydrogen bonding and hydrophobic effect.[2] The stability of these assemblies in solution is mainly due to the hydration of the hydrophilic group and the hydrophobic effect.[2]

The polarity of water molecules causes the partial positive hydrogen and partial negative oxygen, which interact with the hydrophilic group *via* hydrogen bonding. Hydrogen bonds are one of the strongest soft interactions with the interaction energy at *ca.* 120 kJ/mol.[2] The hydrogen bonding between the hydrophilic group and water gains an enthalpy.[2] Many biological molecules have this hydrogen bonding strong enough to bind the assemblies together, but weak enough to be broken apart when needed.[2] In conjunction to hydrogen bonding, the hydrophobic effect is also an essential driving force of surfactant self-assembly.[2] Water molecules can arrange themselves surrounding the hydrophobic group to form a clathrate structure with stronger hydrogen bonds,[2] so a water cavity is created. With the addition of more hydrophobic groups, the hydrogen bonding network of water favors larger cavities to gain entropies by minimizing the disruption of water structure, which is the conventional concept of hydrophobic effects accounting for aqueous self-assembly.[2] The colloidal stability of the resultant assemblies is attributed to the water-solubility of the hydrophilic group.[2]

1.2 Self-assembly of Fp molecules

1.2.1 Introduction to the self-assembly of FpR molecules

Metal carbonyl Fp hydrophobic molecules (Fp = $(PPh_3)(Cp)Fe(CO)(CO\text{-})$) are able to self-assemble in water.[4] As seen in Figure 1, the molecule can be divided into two parts; the Fp polar head and the R non-polar group. Upon self-assembly in water, the Fp head is hydrated and exposed to water with the R non-polar group associated within the interior of the assemblies.[4] The R group in FpR molecules can be varied from alkyl to aromatic groups, which assisted the investigation of the self-assembling behaviour.[5-8]

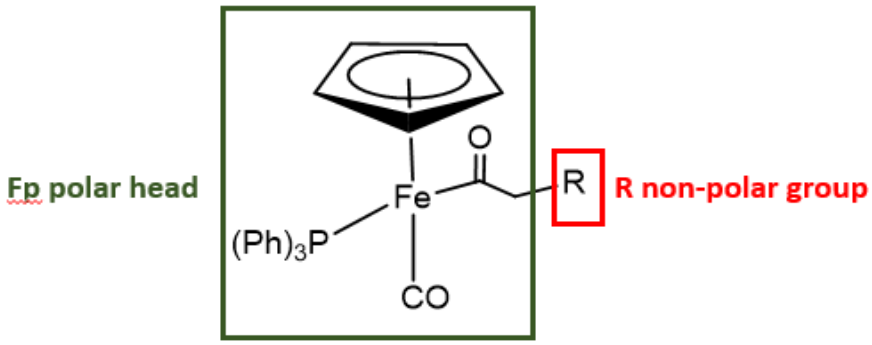

Figure 1: The chemical structure of the metal carbonyl Fp complex.

The first metal carbonyl Fp complex that was synthesized to investigate its aqueous behavior is FpC_6.[4] As seen in Figure 2, the self-assembly of FpC_6 was done by first dissolving 1 mg FpC_6 in THF. MiliQ water (10 mL) was then added into the THF solution to form the colloids. Afterwards, the removal of THF was done by N_2 bubbling, obtaining FpC_6 colloids (0.1 mg/mL) in 100% water.[4] As observed in Figure 1, the blue tint of the solution suggests the formation of colloids.[4] Even with diluting the solution to 0.005 mg/mL, the colloids remain as indicated by the scattering of the green laser (Figure 1).[4] The colloids were subsequently analyzed using dynamic light scattering (DLS), which indicates that the hydrodynamic radius (R_h) of the colloids is *ca.* 85.0 nm with a narrow PDI (0.02). This suggests that the colloids are uniform in size.[4] Static light scattering (SLS) was also performed to investigate the radius of gyration (R_g), which is determined to be 83.6 nm.[4] The R_g/R_h ratio (the shape factor) of 1.0 suggests that the colloids are a vesicular morphology, which was confirmed using cryogenic transmission electron microscopy (Cryo-TEM).[4] The thickness of the vesicle membrane was measured *via* small angle X-ray scattering (SAXS)[4] and atomic force microscopy (AFM) from fragments of the vesicle after drying, which is *ca.* 4.0 nm close to the thickness of the bilayer structure of the FpR molecules.[4] This new group of metal carbonyl bilayer vesicles is named as MCsome.[4]

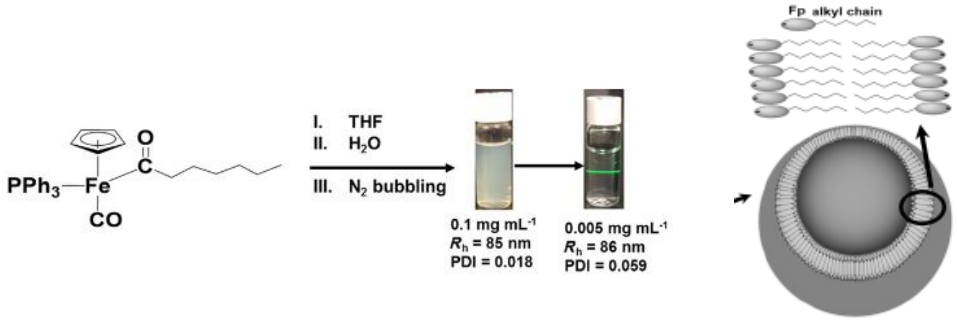

Figure 2: Aqueous self-assembly of FpC_6 and the cartoon for the resultant bilayer vesicular assemblies known as MCsome.[4]

To investigate the assembling behavior of FpC_6 molecules in water, FTIR analysis was done on FpC_6 in THF/water with various water content (v%).[4] The addition of water tends to shift the absorption peaks for the carbonyl groups resulting from the water carbonyl interactions (WCI), which is displayed in Figure 3a. [4] As seen in the figure, the acyl carbonyl group (Figure 3b) is hydrated first at 10 v% in the THF/water mixed solvents.[4] This is due to the higher polarity of the acyl carbonyl group, allowing it to readily interact with water *via* WCI. [4] The DLS analysis of FpC_6 in THF/water as a function of water content is displayed on Figure 3c.[4] As seen in the figure, there is a sudden increase in the count rate as the v% of water reaches 60%, which is an indication of aggregation. [4] This concentration (60%) is known as the critical water content (CWC). When the v% of water is less than 60%, there is no WCI for the terminal carbonyl group (Figure 3b) but becomes hydrated at CWC (60%) as indicated by the redshift of the absorption peaks (Figure 3a).[4] This behavior suggests the aggregation facilitates the WCI, which is caused by a local electric field created by the association of the polar Fp head groups. The local electric field increases the polarity of the terminal CO group and help the WCI.[4] The zeta potential (ζ) of the MCsomes in water was also investigate and measured to be -65 mV, suggesting that the colloidal surface is negatively charged.[4] This is possibly due to the WCIs, since the water interaction with the carbonyl group enhances the partially negative charge of O ($O^{\delta-}$).[4]

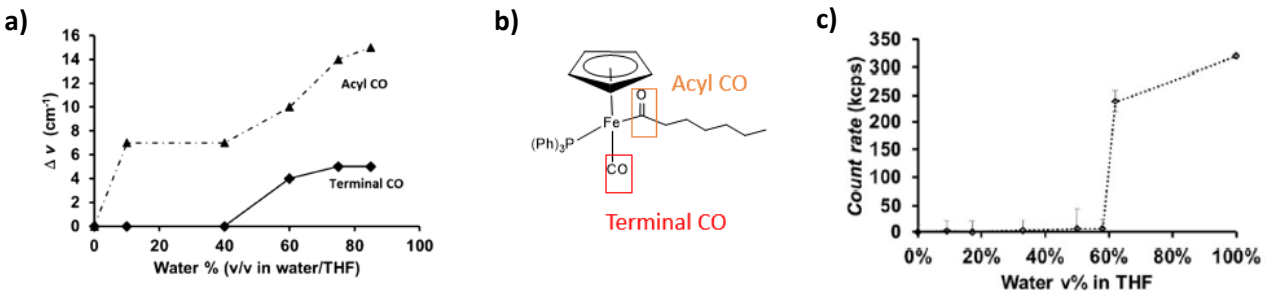

Figure 3: a) The degree of FTIR redshift for the acyl and terminal carbonyl as a function of vol% of water in water/THF solution.[4] b) Chemical structure of FpC_6 with acyl and terminal carbonyl groups highlighted.[4] c) DLS analysis of FpC_6 in in water/THF solution with various vol% of water.[4]

To further investigate the FpR colloids, the effect of the length of the alkyl group on the assembly of FpC_n (n = 1-18) was systematically studied.[5] In the investigation, the FpC_1 colloids in water precipitate after 6 hours indicating that the complex is water insoluble.[5] However, as seen in Figure 4a, the FpC_n colloids with longer alkyl chains are very stable, although the swelling behavior is observed for $FpC_{6\text{-}10}$ colloids.[5] Moreover, there is no swelling for the FpC_{14} and FpC_{18} colloids over several months (Figure 4b).[5] To understand it, CV analysis of FpC_n colloids were performed and a typical data is illustrated in Figure 4c.[5] As shown in the figure, there is an absence of the reduction peak, which is caused by the adsorption of the colloids on the CV electrode upon oxidation.[5] Two oxidation peaks are observed, which is also found in the previous studies of poly(ferrocenylsilane) (PFS) polymers in organic solvents.[5,9] The two oxidation potentials for Fe(II) are caused by the interaction between the two adjacent Fe atoms, where the oxidized Fe makes the adjacent Fe atom difficult to be oxidized and thus requiring a higher potential.[9] The degree of this influence is indicated by the separation of the two peaks, known as voltametric peak separation ($\Delta E_{1/2}$).[9] The $\Delta E_{1/2}$ for FpC_n colloids are compared in Figure 4d. As seen in the figure, the $\Delta E_{1/2}$ decreases as alkyl chain length of FpC_n increases, which is inversely proportional to the distance between two Fp heads (Figure 4d).[5,9] This suggests that there is an increased distance between two Fp heads with longer alkyl

chains.[5] This increased distance creates a cavity where water can fill up the space, which is known as the hydration cavity (Figure 4e).[5] The water in the hydration cavity within the membrane of the colloids could be a contributing factor on stabilizing FpC_n colloids.[5] The interaction of the alkyl groups is detectable by FTIR analysis for the FpC_n assemblies with longer alkyl groups (Figure 4f), but barely detectable for the assemblies with shorter C_n.[5]

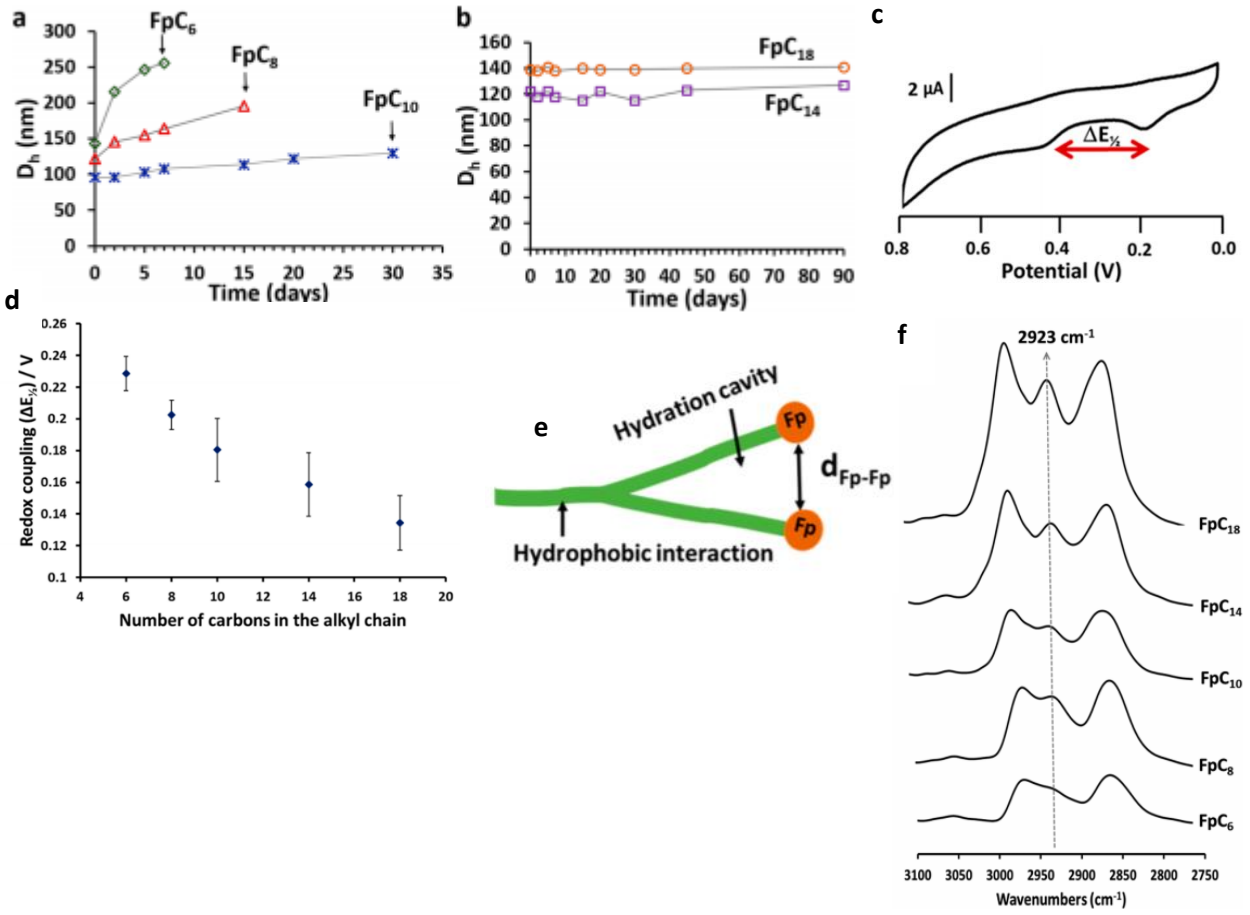

Figure 4: a) The degree of swelling of FpC_n with various C_n after aging for various days. Arrows indicates the time when the FpC_n starts to precipitate.[5] b) The degree of swelling of FpC_{14} and FpC_{18} over time. c) CV analysis of FpC_n colloids, which shows two oxidation peaks that are separated by $\Delta E_{1/2}$.[5] d) Redox coupling as a function of FpC_n alkyl chain length.[5] e) An illustration of the hydration cavity found in FpC_n colloids.[5] f) FTIR analysis illustrating the interaction of alkyl groups.[5]

1.2.2 Structured interstitial water within the membrane of MCsome

To investigate the membrane of MCsome, FpC_6Pyrene MCsome was used due to the fluorescent properties of pyrene groups that associate within the membrane. The fluorescence spectroscopy for the MCsome is displayed in Figure 5a.[10] As seen in the figure, there is a noticeable absence of the excimer peak at 465 nm, which is usually observed for the assemblies of surfactants tagged with pyrene groups due to the hydrophobic interactions.[10] Therefore, the absence of the excimer peak indicates that there is no hydrophobic collapse of the non-polar groups within the membrane of the FpC_6Pyrene MCsome.[10] The non-polar groups are separated by the interstitial water within the membrane, which is confirmed by Raman spectroscopy.[10] Hypothetical addition multivariate analysis with numerical differentiation (HAMAND) has been used to separate the signals for the interstitial water from the bulk water.[10,11] The resultant solute correlated (SC) spectrum is displayed in Figure 5b.[10] As seen in the figure, spectrum for the interstitial water shows a peak at 3250 cm^{-1}, which represent the structured water in terms of hydrogen bonding.[10,11] The intensity for the peak at 3400 cm^{-1} due to the de-structured hydrogen bonding, which is much weaker than that of bulk water. [10,11] This comparison indicates that the interstitial water has a better order of the hydrogen bonds.[10] The peak at 3600 cm^{-1} is attributed to the "dangling" OH group of water that is interacting with the aromatic pyrene group.[10-13] Overall, fluorescence spectroscopy and Raman spectroscopy suggests the formation of structured interstitial water within the membrane of the MCsome that is preventing the hydrophobic collapse of the pyrene group.[10]

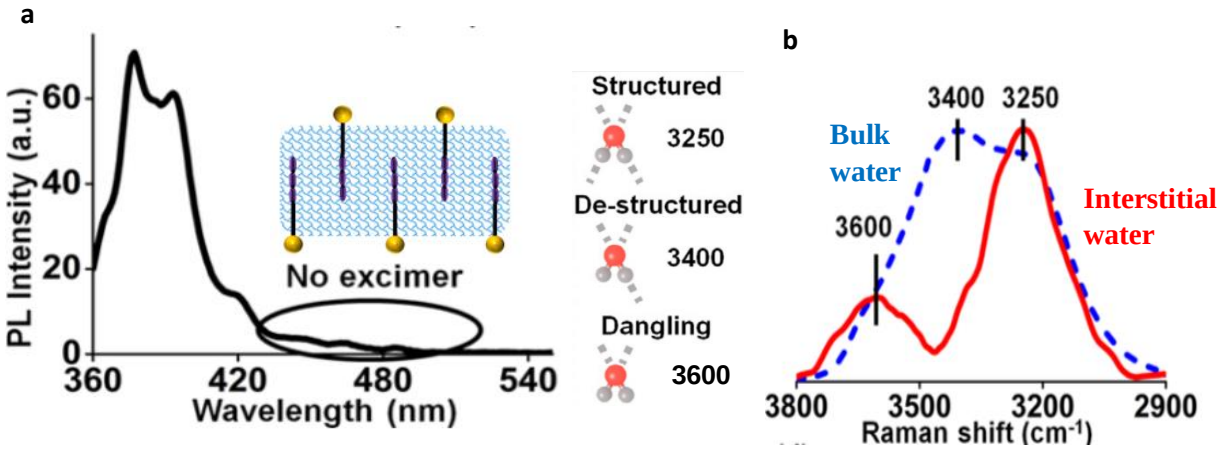

Figure 5: a) Fluorescence spectra of FpC$_6$Pyrene MCsome in water.[10] b) Raman spectra of bulk water (blue) and the SC spectrum of FpC$_6$Pyrene MCsome (red) indicating the difference in water structure.[10]

The influence of the R groups on the interstitial water within the membrane of the FpR MCsome (R = C$_6$Pyrene, C$_3$Bithiophene, C$_6$) was studied. [10] These MCsomes were analyzed using DLS and Raman scattering spectroscopy.[10] Figure 6a display the swelling of the MCsome over 7 days of aging. As displayed in the figure, FpC$_6$ MCsome swells substantially over time as the hydrodynamic diameter (D_h) increases significantly after aging for 7 days in comparison to FpC$_6$Pyrene and FpC$_3$Bithiophene MCsome. [10] To investigate the larger swelling ability of FpC$_6$ MCsome in comparison to FpC$_6$Pyrene MCsome and FpC$_3$Bithiophene MCsome, the interstitial water was studied using Raman spectroscopy. [10] Figure 6b displays the Raman scattering SC spectra for the three FpR MCsome. As seen in the figure, the interstitial water structure is found to be different for different FpR MCsome. [10] To explain, the FpR MCsome have similar structured hydrogen bonding at 3250 cm^{-1}. [10] However, at 3400 cm^{-1}, there is more de-structured hydrogen bonding for FpC$_6$ MCsome in comparison to FpC$_6$Pyrene MCsome and FpC$_3$Bithiophene MCsome, indicating that the interstitial water is less structured. [10] Furthermore, the "dangling" hydrogen is not detectable for FpC$_6$ MCsome. [10] This indicates that there is higher mobility and thus relatively weaker hydrogen bonding for water molecules surrounding the C$_6$ group. [10] This will stimulate an overall weaker hydrogen bonding for the interstitial water *via* hydrogen bonding cooperative effect. [10] In contrast, the pyrene group of FpC$_6$Pyrene MCsome tends to interact more with the "dangling" hydrogen as indicated by

the shorter Raman scattering wavelength at 3600 cm^{-1}. [10] This results in a stronger water interaction with C_6Pyrene, thus reducing the mobility and resulting in stronger hydrogen bonding of the interstitial water. [10] Overall, by analyzing the swelling ability of FpR MCsome and the interstitial water using Raman spectroscopy, it is found that the R-group of the FpR MCsome affect the structural stability of the MCsome. [10] The hydrophobicity and interactions between the R-group and the interstitial water will vary the structure of the interstitial water, thus affecting the swelling ability of the MCsome. [10]

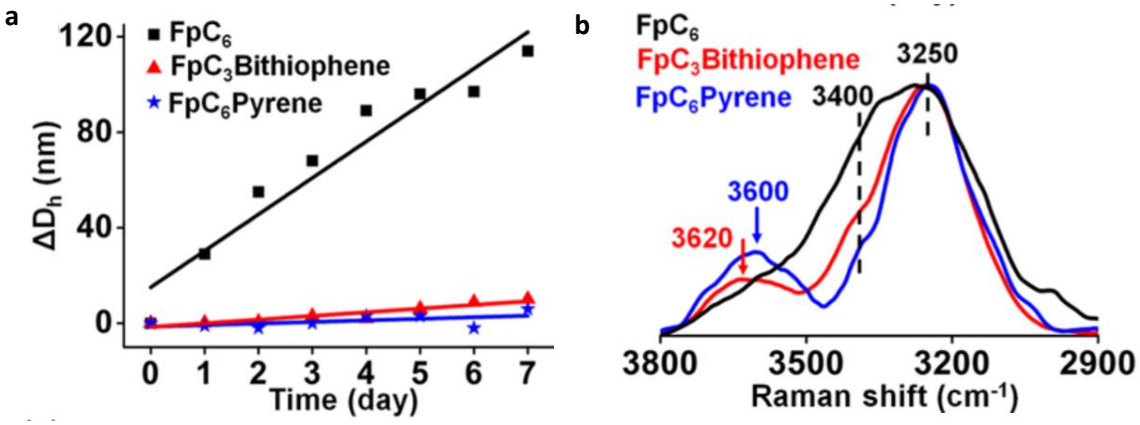

Figure 6: a) DLS analysis of FpR MCsome to investigate the swelling behavior over time.[11] b) Raman spectroscopy of FpC_6 (black), FpC_3Bithiophene (red), and FpC_6Pyrene MCsome (blue), which indicates the differences in their interstitial water structure.[9]

The consequence of aging MCsome on the interstitial water was studied by using FpC_6 MCsome. Figure 7 displays the SC Raman spectrum for FpC_6 MCsome aged for 7 days that is compared with the spectra for the freshly prepared the MCsome and bulk water. [10] As seen in Figure 7, the freshly prepared FpC_6 MCsome has well-structured hydrogen bonding as indicated by stronger peak at 3250 cm^{-1} in contrast to the de-structured hydrogen bonding peak at 3400 cm^{-1}. [10] However, after aging for 7 days, there is a decrease in the peak at 3250 cm^{-1} and an enhancement of the peak at 3400 cm^{-1}, suggesting that the interstitial water structure changes from structured to de-structured hydrogen bonding over time. [10] This is due to the increase in swelling of the MCsome, thus allowing for the de-structured water to gain entropy. [10]

Furthermore, a peak is visible at 3640 cm^{-1} that suggests the occurrence of the "dangling" hydrogen, and a peak visible at 3640 cm^{-1} that suggests the formation of clathrate-like water structure surrounding the alkyl group. [10] Therefore, Raman spectroscopy suggests that the aging MCsome results in the change in the interstitial water of the MCsome, which is responsible for the structural integrity of the MCsome, thus resulting in its swelling behaviour. [10]

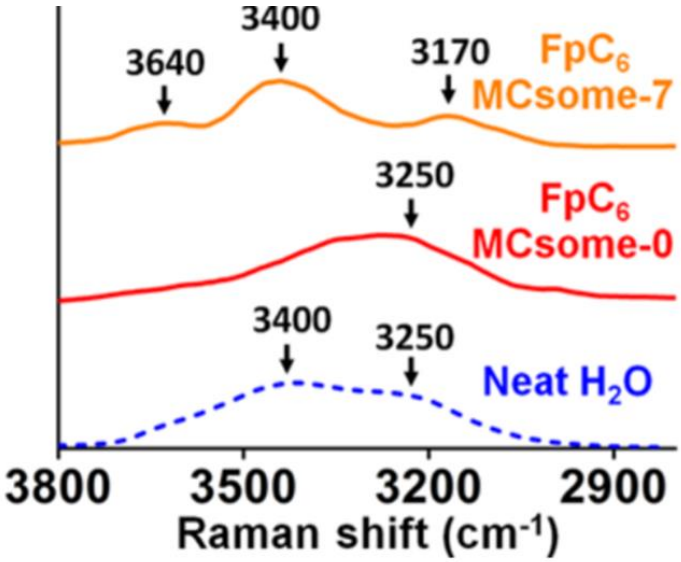

Figure 7: Raman spectroscopy of FpC_6 MCsome aged for 7 days (orange), freshly prepared FpC_6 MCsome (red), and bulk water (blue). [10]

1.2.3 Investigating the interstitial water using bithiophene group as a probe

The bithiophene (BT) group consist of two thiophene aromatic rings that are connected by a covalent bond and is capable of intramolecular rotation.[16] BT molecules emits fluorescence, in which the fluorescence intensity is dependent on the intramolecular motion and intermolecular interaction. The restriction of the intramolecular rotation reduces the energy dissipation, which helps the emission of fluorescence. The association of rotation-restricted pyrene groups possibly results in an intermolecular conjugation,[16] which is influenced by the conformation of the BT groups.[16] The planar pyrene groups help the conjugation that is another pathway for the energy dissipation and thus reduces the intensity of fluorescence (Figure 8).[16] In contrast, the conjugation does not occur for the associated torsional BT groups (Figure 8), which reduces the energy dissipation and the fluorescence will be stronger.[16]

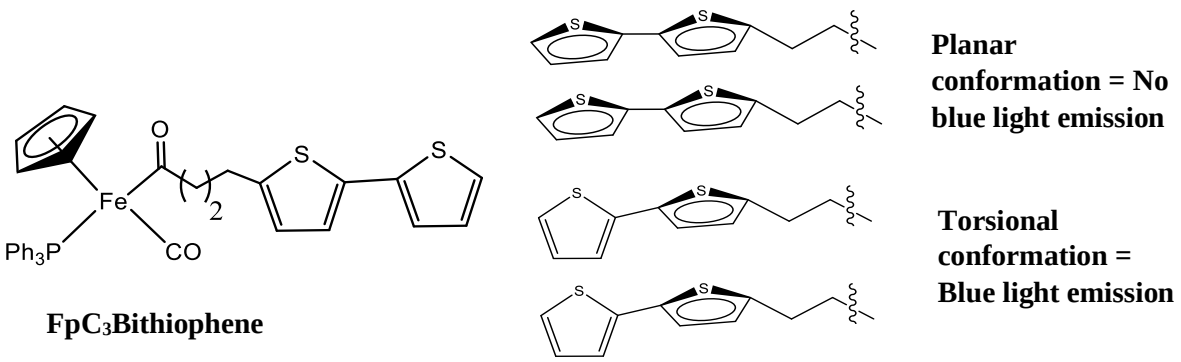

FpC$_3$Bithiophene

Figure 8: FpC$_3$Bithiophene and possible conformations for bithiophene.

FpC$_3$Bithophene MCsome has a vesicular membrane, which is constructed from bithiophene groups with interstitial water. By examining the fluorescence, it is possible to study the interstitial water, including its capability for the restriction of the intramolecular rotation and intermolecular conjugation.[16] This was studied by subjecting FpC$_3$Bithiophene MCsome to various solution conditions. [16] As seen in Figure 9, FpC$_3$Bithiophene MCsome in THF/water solution was found to be in its torsional conformation as indicated by UV-Vis analysis and the colloids emit strong blue fluorescence. It suggests the interstitial aqueous media of THF/water can restrict the intramolecular rotation and prevent the intermolecular conjugation due to the torsional conformation.[16] The removal of THF from the solution using N_2 bubbling and subsequently adding THF back to the solution does not substantially affect the fluorescence. It suggests the N_2 bubbling does not influence the restriction of the intramolecular rotation, which is verified by UV-Vis spectroscopy.[16] In contrast, when the THF is removed by dialysis, the conformation of the bithiophene group converted to planar conformation as indicated by the UV-Vis spectra and the resultant solution in water barely emit blue fluorescence.[16] The change in conformation is explained by the osmotic pressure of dialysis.[16] When the dialyzed FpC$_3$Bithiophene MCsome in water was irradiated with UV light (365 nm), no intramolecular rotation occurs as indicated by UV-Vis analysis and no enhanced intensity of the blue emission is observed. This result suggest that the interstitial water has a strong force to restrict the intramolecular rotation and the planner bithiophene groups have an effective intermolecular conjugation to dissipate energy. As the bithiophene groups in the vesicular membrane are separated by interstitial, the conjugation without direct

molecular interaction is known as through space conjugation. The role of water may play a role in the conjugation, which is the issues studied in this thesis. The addition of THF back into the dialyzed FpC_3Bithiophene MCsome does not vary the UV-Vis and FL spectra substantially, suggesting no conformation change of the bithiophene groups. The resultant solution in THF/water was then irradiated by the UV light, and the rotation of the bithiophene groups from planner to torsional conformation was found. Consequently, the solution emits blue fluorescence.[16] It is explained by the reduced cohesive energy of the aqueous media upon the addition of THF to the water solutions. Overall, the fluorescence of the FpC_3Bithiophene MCsome at various solution conditions illustrates the interstitial aqueous media, including THF/water and water, can restrict the intramolecular rotation, which may induce through space conjugation or not depending on the bithiophene conformations.[16]

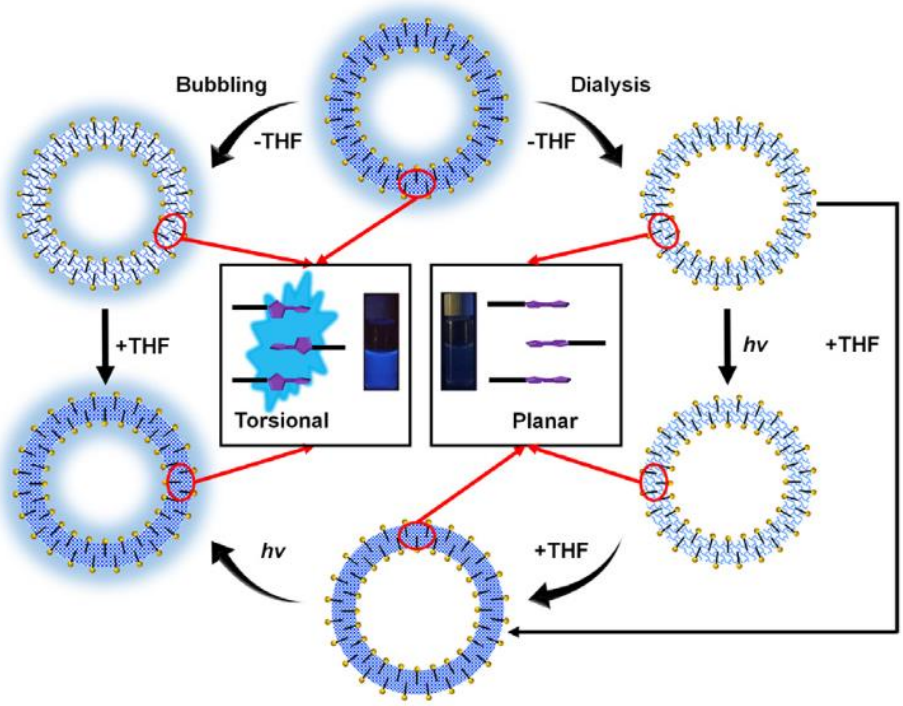

Figure 9: FpC_3Bithiophene MCsome under different conditions. The presence and absence of the blue light emission of the BT groups suggests its confinement in the interstitial water depending on its fixed conformation. [16]

1.3 Introduction to nano-confined water and its presence in self-assembly

The confinement within nano-space has been found to influence the structural and dynamics of water, which can be different compared to bulk water. [17,18] The structure and dynamics of the water molecules is dependent on the size of the confinement space and its surrounding environment.[17,18] Computer simulation is the major tool for the investigation of nano-confined water. [19,20] Water confined within carbon nanotubes (CNTs) is one system that have been studied. Chakraborty et al. investigated the confined water in CNTs using pair correlation function, which measures the variation in density of the confined water as a function of the distance from a reference point. [20] As seen in Figure 10a, the well-defined sharp peaks indicates that the water molecules are well ordered within the CNTs of various lengths.[20] Furthermore, the confined water in CNTs have a strong anisotropy,[20] which suggests that the orientational relaxation (relaxation of hydrogen bonding) is much faster in contrast to bulk water. This indicates that the confinement speeds up the water dynamics. [20] This nano-confinement effect was explained by the angular jumps of the confined water molecules, which is investigated by Mukherjee et al. using molecular dynamic simulations. The angular jump (as seen in figure 10b) is the change in orientation of the water molecules depending on the most thermodynamically stable orientation. The water confined within nanotubes is in a single-file chain, which facilitates the angular jump of water molecules between two stable states and thus increases the water dynamics (Figure 10b).[21] The consequence of increased water dynamics is that there are less hydrogen bonding thus allowing for the spontaneous entry of water molecules into the hydrophobic cavity of CNTs. [20] The increase in rotational entropy within the confined water of CNTs allowed for the water molecules to stay within the hydrophobic regions of CNTs because it is thermodynamically favorable.[20]

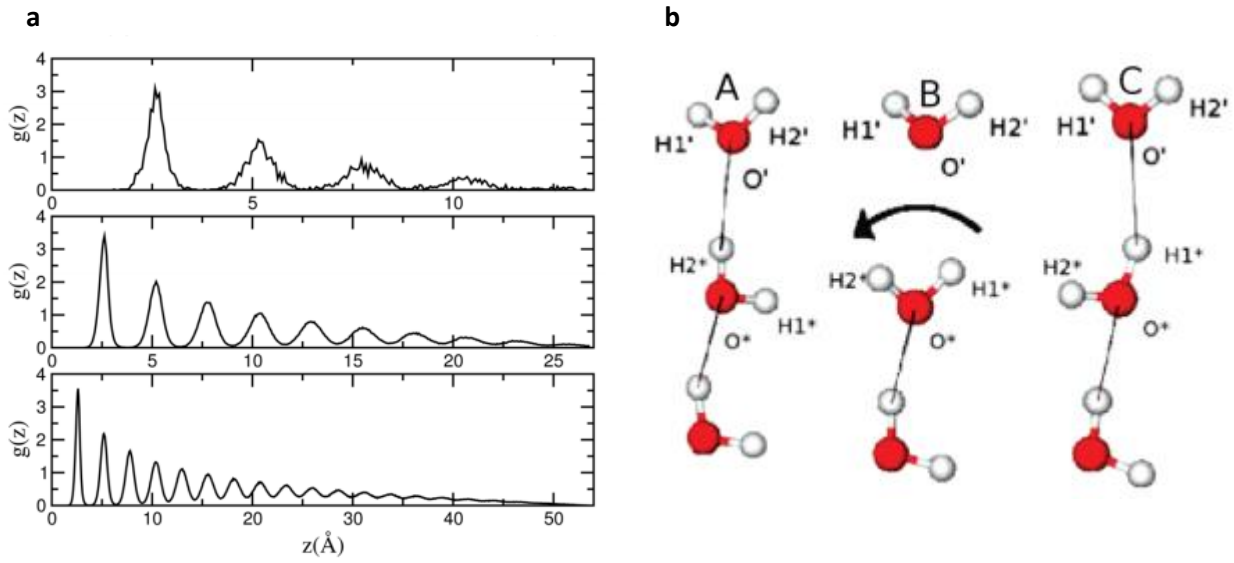

Figure 10: a) The pair correlation function of confined water within CNTs of various lengths (14, 28, and 56 Å top to bottom).[20] b) A model illustrating the angular jump of confined water within CNTs.[21]

The phase transition between liquid water and ice is different in nano-confined water in comparison to bulk water. The ice-liquid oscillations in nano-confined water were studied by Kastelowitz et al. using molecular simulations. [22] As seen in Figure 11a, it was found that the nano-confined ice can structurally exist in a bilayer hexagonal structure. [22] This bilayer structure was previously found to have a high melting temperature, which was investigated through molecular simulations that produced a phase diagram in comparison to the bulk hexagonal structure in ice. [23] This was further proven by the analysis of the time evolution of the number of ice molecules in confined water at 278.75 K as seen in Figure 11b.[22] As seen in the figure, the number of ice molecules that exist in confined water oscillates over time.[22] This suggests that the confined water exists either as an all-liquid state or an all-ice state as illustrated in Figure 11c. [22] To investigate this, a free energy profile was computed depending on the number of ice molecules in the confined water. [22] As seen in Figure 11d, nano-confined water is not able to coexist between the crystal and liquid states but oscillate between the two phases in equilibrium. [22] This is due to the smaller energy barrier that is needed to cross between the two phases, which is sensitive to thermal fluctuation. [22] This is evident in the change in free energy needed to cross the barrier at different temperatures displayed in Figure 11d. [22]

In contrast, bulk water in a macroscopic scale cannot oscillate between crystal and liquid states because the energy barrier is too great to be overcome by thermal fluctuation. [22] This suggests that the nano-confined water affects the phase coexistence of its various states.[22]

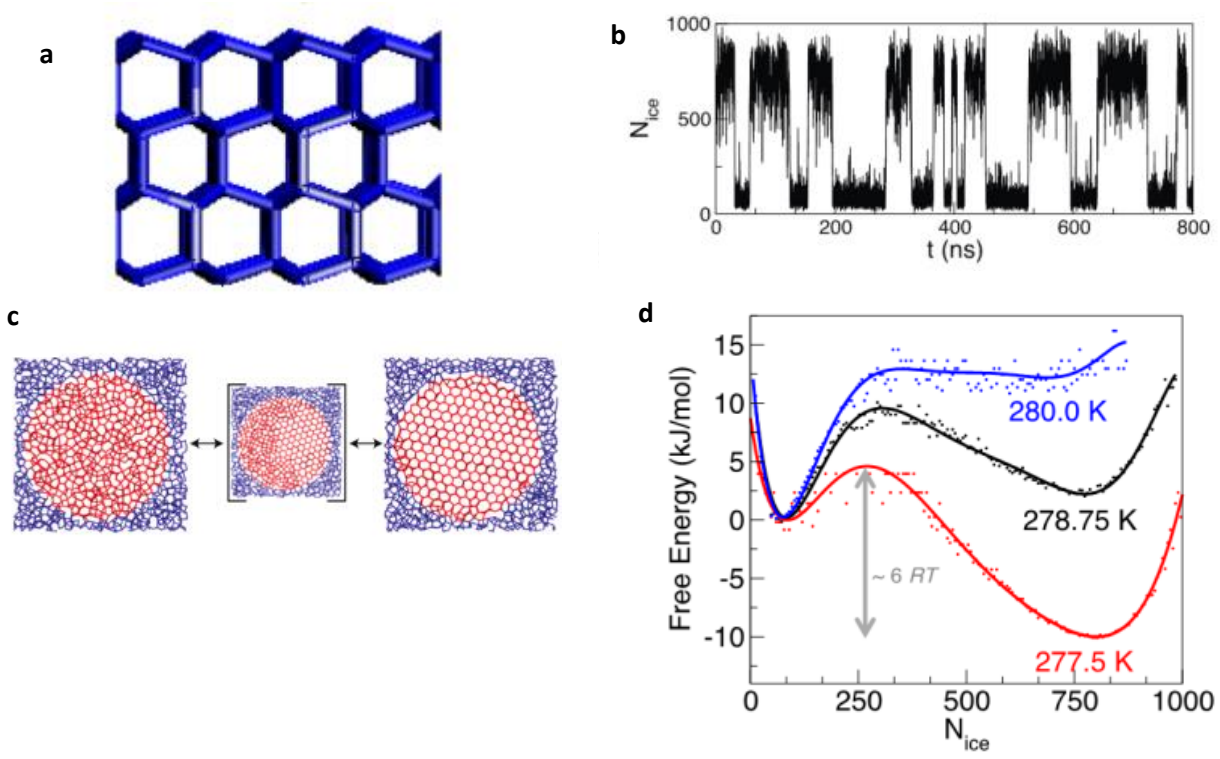

Figure 11: a) A model of the hexagonal bilayer structure of nano-confined water. [22] b) The time evolution analysis of number of ice molecules in nano-confined water at 278.75 K. [22] c) An illustration showing the transition of nano-confined water from an all-liquid state to an all-ice state with a mixture between both states as an intermediate. [22] d) Free energy diagram of nano-confined water with respect to the number of ice molecules.[22]

Nano-confined water is also found in surfactant assemblies, which are found in the hydrophobic regions of the assemblies.[24] Hanot et al. investigated the impact of water on the morphology of ionic surfactant assemblies. [24] The hydration conditions that affect the morphology of these assemblies was investigated by subjecting the surfactants in different amounts of water content. [24] A model was produced

using calculated measurements of columbic interactions as displayed in Figure 12a. [24] As seen in the figure, at hydration level (λ) of 0, the surfactants form an irregular lamellar shape with the non-polar groups interacting with each other while the polar group interacts with the hydronium ions. [24] Increasing the λ to 4 allows for the formation of well-ordered lamellar structures where water is found to interact with the polar head. [24] When the λ increases to 12, the lamellar structure starts to form a cylindrical type of structure while further increasing the λ to 32 allows for the formation of micelles. [24] This transition of assembly morphology is attributed to the C_0 of the morphology where an increase in water content decreases the concentration of the surfactant, thus changing the morphology. [24] However, they became curious to see how water interacts with the surfactant at different water content. [24] To further study this, the average coordination number of water molecules (n_w) in the assemblies was plotted, which is dependent on λ, as seen in Figure 12b. [24] As seen in the figure, at a high λ, the n_w is like bulk water. [24] There is a slight decrease in n_w when λ decreases to 6. [24] This corresponds to the formation of the well-ordered lamellar structure. [24] At $\lambda < 3$, the n_w is found substantially decrease until $n_w = 1.2$. [24] This is related to the hydronium interaction with the polar head at λ = 3 where water can replace the hydronium ion. [24] To investigate further, the n_w is then plotted against the distance from the nearest hydrophilic head, which would be the interface of the assembly. [24] As seen in Figure 12c, for all λ, the n_w increases with increasing the distance from the nearest hydrophilic head. [24] This suggests that the water closest to the interface has less n_w. [24] Furthermore, when the λ = 32, 3 regions of water inside the ionic domain (polar region of the assembly) can be highlighted. [24] The first region is the bulk-like interface, which is located farthest from the hydrophilic head. [24] This surrounds the ionic domain of the surfactant and resembles properties of bulk water, which is shown by the n_w like water. [24] The second region is the intermediate interface, which is located about 6 Å from the hydrophilic head. [24] This area is known for the layering of water molecules, thus allowing for high n_w in lamellar structures. [24] Lastly, the third region is the interface-limited region, which is located closest to the hydrophilic head. [24] The water in this region is nano-confined to the point where its properties do not resemble those of bulk water. [24]

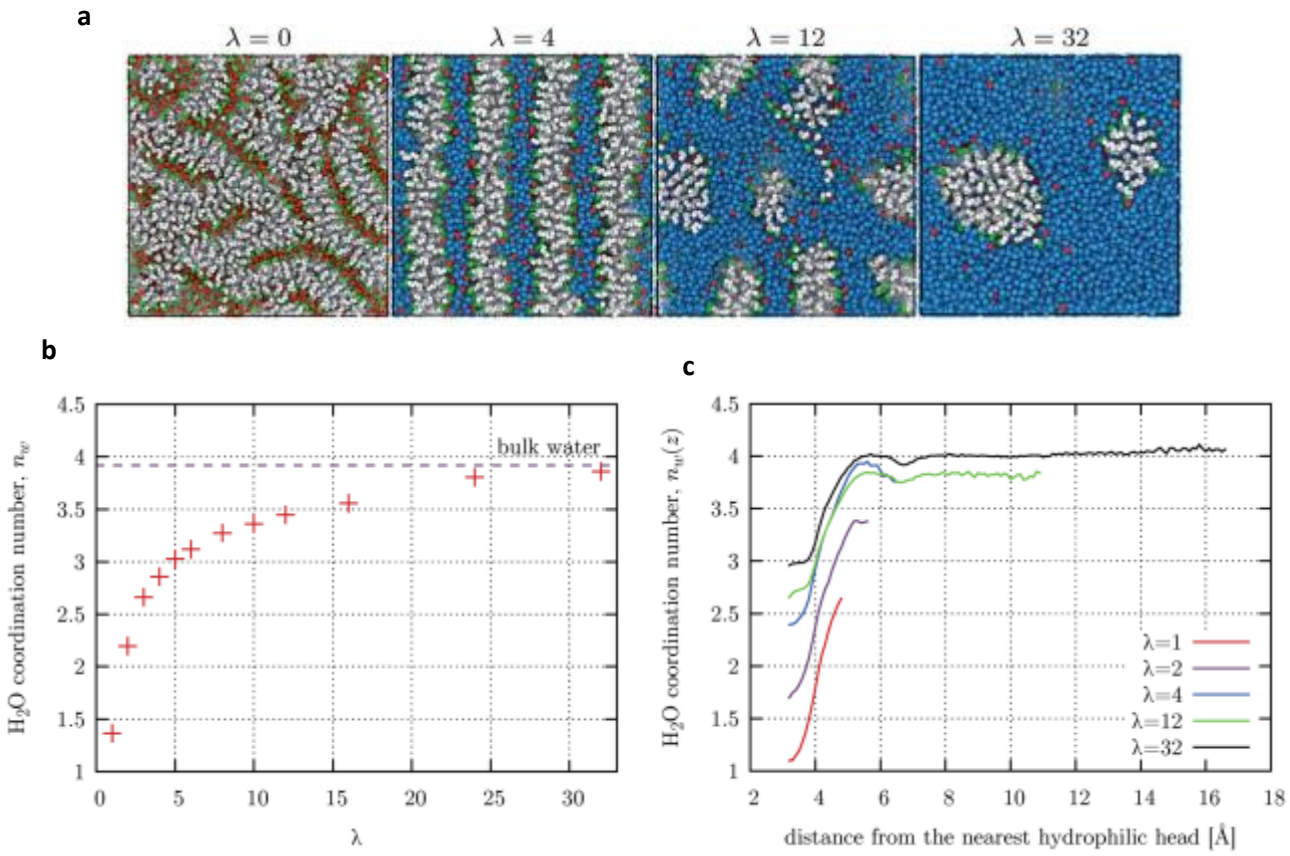

Figure 12: a) The model of the surfactant assemblies showing different interactions at different λ (grey = non-polar group, green = sulfate polar head, blue = water, and red = hydronium ion). [24] b) A plot of the n_w against λ. The dotted line represents bulk water. [24] c) A plot of n_w corresponding to the distance from the nearest hydrophilic head at different λ. [24]

Reverse micelles are the droplets of water stabilized by surfactants in organic media. [25] As seen in Figure 13a, the polar head of the surfactant interacts and encapsulates the water within the core of the micelle while the non-polar tail is exposed to the non-polar solvent. [25] The core of the reverse micelle contains nano-confined water. [25] The encapsulation of the nano-confined water was studied by Moilanen et al. to investigate the dynamics of nano-confined water in reverse micelles. Aerosol-OT (AOT) and Ipegal were used as the surfactants. [26] Time-dependent IR anisotropy measures the orientational relaxation dynamics of water *via* the decay of OD stretching. [26] The dynamics of nano-confined water within reverse

micelles comprised of nonionic and ionic surfactants with 5% HOD in H_2O were measured and compared with bulk water. [26] As seen in Figure 13b, the anisotropy decay of nano-confined water in both AOT and Ipegal reverse micelles is much slower in comparison to bulk water. [26] This suggests that the orientational dynamics of water is much slower in the reverse micelle core in comparison to bulk water. [26] Moreover, AOT is a cationic surfactant while Ipegal is a nonionic surfactant. [26] As displayed in Figure 13b, the anisotropy decay of both AOT and Ipegal are like each other, suggesting that the polarity of the head group does not significantly influence the nano-confined water dynamics of reverse micelles. [26] Further research done in this topic demonstrates that the size of the reverse micelle can influence the nano-confined water dynamics. [27] AOT reverse micelles of different sizes with desired water molecules per AOT molecule (w_0) were prepared in where a smaller micelle would produce a smaller w_0. [27] These micelles were also analyzed using time-dependent IR anisotropy as shown in Figure 13c. [27] As seen in the figure, as the w_0 of the AOT increases, the orientational relaxation of the nano-confined water increases. [27] This suggests that the orientational relaxation of the nano-confined water is influenced by the w_0 present, which is dependent on the size of the reverse micelle. [27] With larger reverse micelles, the nano-confined water resembles water dynamics like bulk water. [27] As the size of the reverse micelles decrease, the reorientation of the water molecules and the structural change of the interface begin to slow down the dynamics of the water due to its increased confinement. [27] It is noted that the dynamics of the water confined within CNTs are different in comparison to reverse micelles. This could suggest that the confinement system of the nano-confined water is crucial and influences the water dynamics. It may be due to the environment surrounding the nano-confined water since confined water in CNTs are in a non-polar environment while confined water in reverse micelles are in a polar environment. This could influence the interactions between the water molecules and the environment, and between other water molecules.

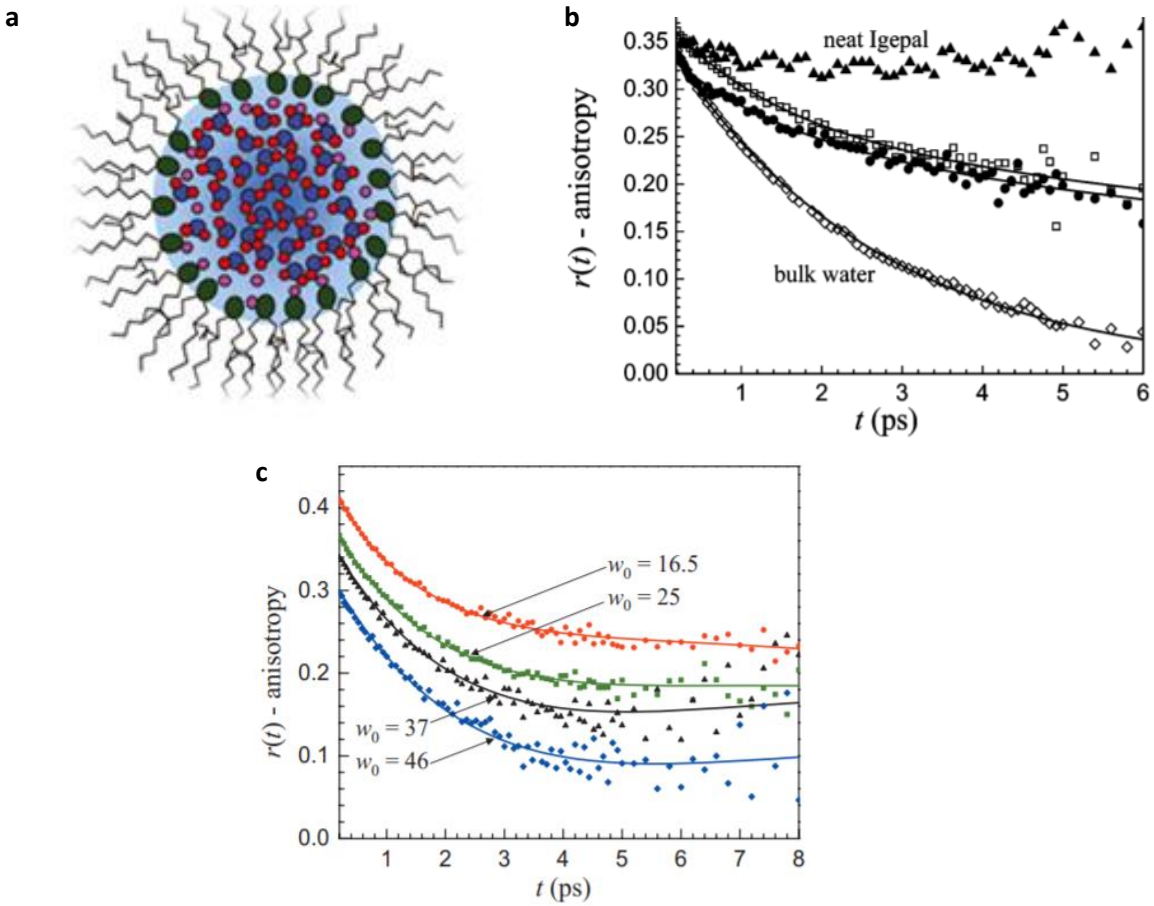

Figure 13: a) Structure of a reverse micelle. The polar head encapsulates the water while the non-polar alkyl group is exposed to the non-polar solvent.[25] b) Orientational relaxation of nano-confined water in Ipegal reverse micelle (circle) and AOT reverse micelle (square), in contrast to bulk water (diamond) and neat Ipegal (triangle).[26] c) Orientational relaxation of nano-confined water in AOT reverse micelles with different w_0.[27]

The confined nano-confined water within biological systems have also been studied. The water in protein crystals is different compared to bulk water because it is confined by the crystalline arrangement of the protein molecules.[28] Water within the surface of proteins tend to have different behaviours at lower temperatures in comparison to bulk water.[28] Water molecules in the first hydration shell of proteins do not crystallize when the temperature is lowered.[29] This has been previously researched by Doster et al., which used IR spectroscopy to determine the glass transition of water in myoglobin crystals.[29] With this prior

knowledge, Weik et al. used confined water within proteins to study its relation to protein dynamics in *Torpedo californica* acetylcholinesterase (TcAChE). [28] TcAChE was found to de-structure at around 100 K. [28] Therefore, they were curious on the relationship between water and protein dynamics around the glass transition temperature of TcAChE, which was investigated using Fournier mapping and X-ray irradiation to induce structural changes at 155 K (water glass transition temperature in TcAChE) and 100 K. [28] Fournier mapping can show the changes in electron density within the structure of a protein, which indicates a possible change in the structure. [28] As seen in Figure 14a, the red cage around the carboxyl group of Glu199, which represents the loss in electron density that could be due to the decarboxylation of Glu199 after X-ray irradiation. [28] However, as seen in Figure 14b, the green cage above His440 shows a gain in electro density while a red cage also surrounds His440, which indicates a conformational change possibly due to the decarboxylation of Glu199. [28] This conformational change at 155 K corresponds with the glass transition temperature of water in TcAChE, which suggests that the glass transition of water in the protein can enhance the protein's local flexibility. [28] This demonstrates the importance of nano-confined water, and their potential uses to understand complex systems such as proteins. [28]

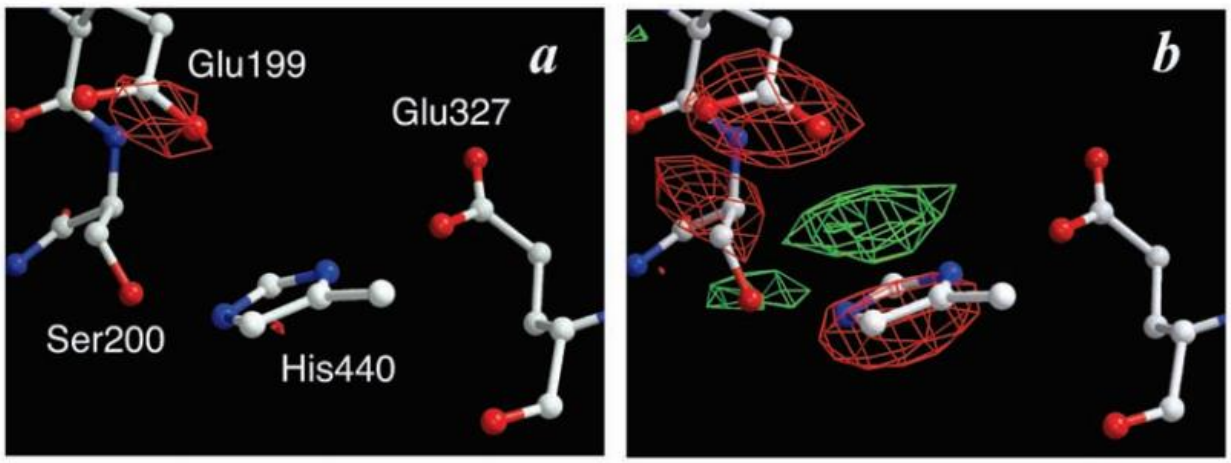

Figure 14: Fournier mapping of the active site of TcAChE at a) 100 K and b) 155 K.

1.4 Research objective

The objective of this research is to investigate the water confined within the self-assembled membrane of MCsomes. The research takes advantage of the aromatic groups tagged on the FpR building blocks that assembled into MCsome. The optical properties of the aromatic groups associated within the membrane are responsive to the external environment, by which the interstitial water can probed and studied.

2. Preparation parameters for the aqueous FpR MCsome

This chapter describe the experimental details and discuss some preparation factors that influence the self-assembling behavior of FpR colloids. These factors include the quality of water used to prepare and dialyze the colloids, the order of mixing water and the THF solution of FpR molecules, and the rate of adding water to the THF solution of FpR.

2.1 Experimental

2.1.1 Synthesis of FpR molecules

The synthesis of FpC_6Pyrene was done by reacting the Fp anion with BrC_6Pyrene in THF at 0 °C with stirring. After 30 minutes, the temperature was then raised to 25 °C and stirring was continued for 1 hour. Using the migration insertion reaction, triphenylphosphine was added and the solution was refluxed at 70 °C for 72 hours. The solution was then cooled to room temperature and the removal of THF was done under vacuum. The golden-brown solid was then chromatographed using a silica column with THF as the eluent. The yellow band was collected, and the solvent was removed using a rotary evaporator. FpC_6 and FpC_6Azobenene are synthesized in the same fashion. This synthesis has been reported in previous research.[7,10]

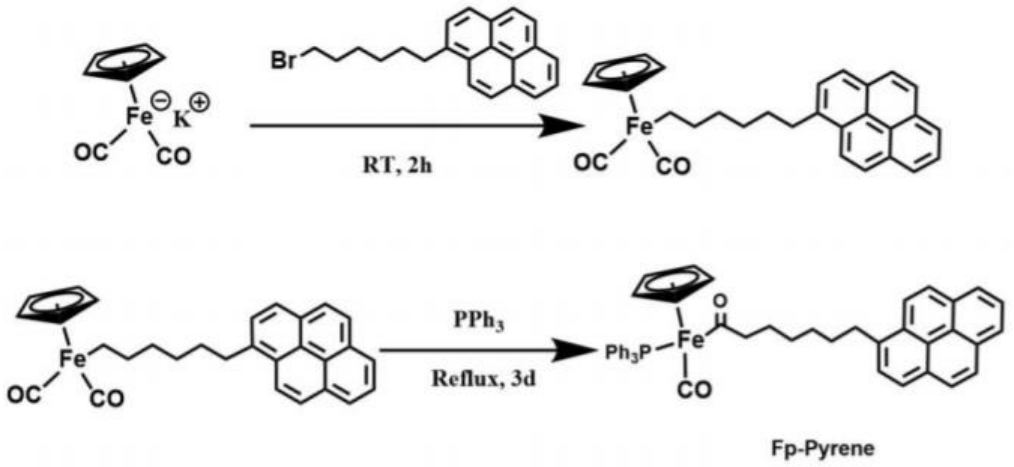

Figure 17: The scheme for the synthesis of $FpC_6Pyrene$.[7]

2.1.2 Preparation of $FpC_6Pyrene$ MCsome

Firstly, 1 mg of $FpC_6Pyrene$ was weighed out into a vial and subsequently dissolved with 0.89 mg of THF (to account for density: THF = 0.89 g/mL) to obtain a concentration of 1 mg/mL of $FpC_6Pyrene$ in THF. To form the MCsome, 9 mL of MilliQ water was added to the solution to obtain the overall concentration of 0.1 mg/mL of $FpC_6Pyrene$ MCsome in a 1:10 volume ratio of THF:water. The $FpC_6Pyrene$ MCsome was subsequently transferred into a cellulose based dialysis tube. The dialysis was done over a period of 24 hours and the water was changed at the 0.5-hour mark, 2-hour mark, and 4-hour mark to remove the THF from the dialysis water.

2.2 The factors influencing the preparation

2.2.1 The effect of water on the preparation of $FpC_6Pyrene$ MCsomes.

The MiliQ water aged in air for various times were used to mix with the THF solution of $FpC_6Pyrene$ for the preparation of the colloids. The resultant colloids in water/THF solution were analyzed by using DLS. The D_h of the MCsome prepared from the MiliQ water aged for 24 hours, 5 days, and 5 months is 129 nm, 142 nm, and 192 nm, respectively. This significant difference in D_h depending on the aging time suggests that the quality of the MiliQ water is an important factor. A possible factor influencing the quality of the MiliQ water is the increase in acidity. The absorption of carbon dioxide as water aging in

air is a possible reason, which changes the pH of water. Therefore, fresh MiliQ water is used for the following study.

The distilled water available from the lab faucet was used for the dialysis of FpC_6Pyrene MCsomes to remove THF. Conductivity of the distilled water is found to be 12 μS, which is slightly higher than regular distilled water (0.5 - 8 μS). To investigate whether the conductivity of the water influence the self-assembly, two samples of FpC_6Pyrene MCsomes in THF/water were prepared by adding fresh MiliQ water to the THF solutions, followed by dialysis using distilled water (12 μS) without and with the addition of salt (100 μS), respectively. The D_h from these two solutions change from 194 nm and 205 nm to 163 nm and 150 nm after the dialysis. It appears that the conductivity of the water used for dialysis does not affect the D_h substantially. Therefore, the distilled water is used for further studies.

2.2.2 The order of mixing water and the THF solution of FpR.

Water and the THF solution of FpC_6Pyrene molecules were quickly mixed for the preparation of the colloids, which was performed by either adding water into the THF solution (Method A) or adding the THF solution into water (Method B). The resultant colloids in THF/water solution were analyzed using DLS. As shown in Table 1, the D_h is 207 nm and 161 nm for FpR MCsome prepared using Method A and Method B, respectively. It is obvious that the addition of water into the THF solution (Method A) produces larger colloids. This pathway dependent self-assembling behavior suggests that the self-assembly creates kinetic colloids.

Table 1: The analysis of D_h and PDI, and the calculation of I_1:I_3 ratio of FpC_6Pyrene MCsome prepared by using different methods.

FpC_6Pyrene MCsome preparation	D_h / PDI / I_1:I_3 ratio
Method A (Water added into the THF solution)	207 nm / 0.13 / 1.71
Method B (the THF solution added into water)	161 nm / 0.10 / 1.84

As the colloids assembled from the molecules containing pyrene groups, which emit fluorescence and can be used to probe the aqueous environments. The spectra for the two solutions are displayed in Figure 15. As shown in the figure, the fluorescence intensity for the colloids prepared by Method A is

relatively weaker, suggesting the two preparation methods created different aqueous environments. The polarity of the aqueous environment can be estimated by the I_1: I_3 ratio, which is the comparison of the fluorescence intensity at 375 nm with 385 nm.[30] A higher ratio indicates a higher polarity. As seen in Table 1, the I_1: I_3 ratio for the colloids prepared by Method A is 1.71, which is lower than those prepared by Method B (1.84). This difference further confirms the aqueous environments around the pyrene groups is variable depending on how water and the THF solution is mixed. This difference will be studied in Chapter 3.

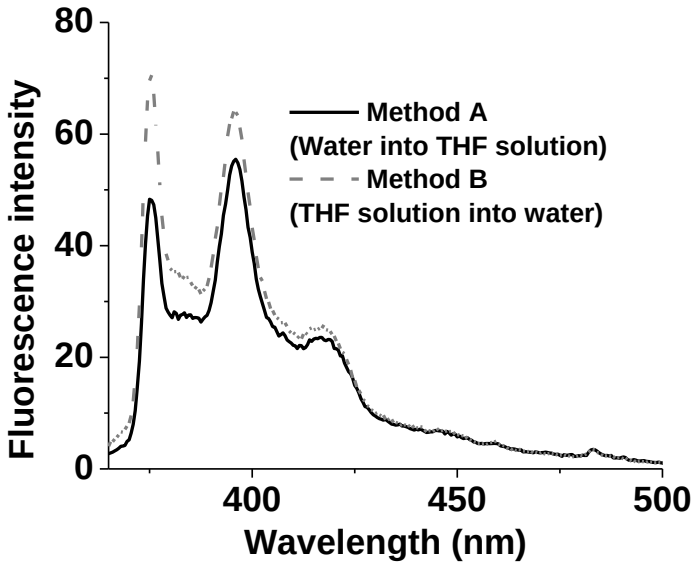

Figure 15: Fluorescence spectra for the FpC_6Pyrene MCsomes in water/THF solution prepared by either adding water into the THF solution (Method A) or adding the THF solution to water (Method B).

2.2.3 The effect of water addition rate into the THF solution of FpR.

The self-assembling behavior is influenced by the water addition rate in Method A. We prepared FpC_6Py colloids in THF/water (1/10 by volume) by either adding MiliQ water (10 mL) to the THF solution (1 mL) instantaneously or dropwise (1 drop per second). The resultant colloids were analyzed by using DLS and fluorescence spectroscopy. As shown in Table 2, the slower addition of water creates larger colloids with a more polar aqueous environment surrounding the pyrene groups. Moreover, as seen in

Figure 16, the fluorescence intensity is significantly higher than that emitted from the colloids prepared from the quick addition of water. This experiment further confirms that water is an active component involved in the kinetic self-assembly, whose role is dependent on the preparation methods and is yet to be explored.

Table 2: The analysis of D_h and PDI, and the calculation of I_1:I_3 ratio of FpC_6Pyrene MCsome prepared by adding water into THF solution at different rates.

Addition of MiliQ water	D_h / PDI / I_1:I_3 ratio
MiliQ water added quickly	156 nm / 0.142 / 1.76
MiliQ water added dropwise (1 second/ drop)	348 nm / 0.109 / 2.42

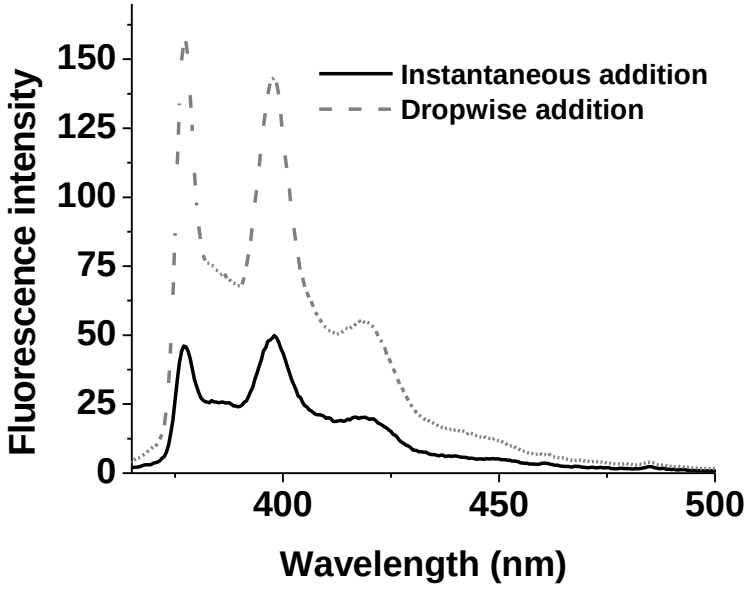

Figure 16: Fluorescence spectra of FpC_6Pyrene MCsome in water/THF solution prepared by adding water into THF solution at different rates.

2.3 Experimental procedure for temperature-dependent constructional water within MCsome

Based on the above preliminary exploration, we became curious as to what other factors can influence MCsome. Understanding that MCsome are sensitive to its solution conditions, it is possible that temperature can also be a factor that affects MCsome. The temperature effect on water dynamics has been well-established.[31] However, the temperature effect on confined nano-confined water is not fully

understood as most research done in this area have been focused on computer simulations.[20,22,23,28] Therefore, we became curious as to how temperature will affect the interstitial water of MCsome. Moreover, as water is a component for structural integrity of MCsome, we predict that the temperature effect on the interstitial water will have a profound effect on the structural integrity of MCsome.

2.3.1 Changing the temperature of FpC_6Pyrene MCsome

To investigate the temperature effect on FpC_6Pyrene MCsome in water, the MCsome was exposed to different temperatures. The MCsome in water was initially prepared at 25 ℃ after 24 hours of dialysis to remove THF……. The solutions were cooled to 6 ℃ or heated to 40 ℃, 50 ℃, and 70 ℃, and subsequently aged at the corresponding temperatures for 24 hours or 5 days before the measurement.

2.3.2 Dynamic light scattering

The FpC_6Pyrene MCsome were analyzed using DLS to investigate the change in size *via* temperature effect. The Malvern Zetasizer Nano S-90 instrument was used with a laser wavelength of 633 nm at a fixed angle of 90° to measure the MCsome. Due to the temperature effect on the viscosity of water, the viscosity setting in the dispersant option was changed depending on the temperature needed for analysis.

2.3.3 Analysis of the interstitial water using fluorescence spectroscopy

To investigate the temperature effect on the interstitial water of MCsome, the FpC_6Pyrene MCsome were analyzed using fluorescence spectroscopy. The Perkin Elmer Luminescence Spectrometer LS 50 B was used to measure the fluorescence of the MCsome. An excitation wavelength of 340 nm was used with a wavelength range of 360 nm to 550 nm, and a slit width of 2.5 was used. A quartz cell with a light path of 1 cm was used.

2.3.4 Analysis of azobenzene isomerization using UV-Vis spectroscopy

To investigate the temperature effect on the cohesive strength of the interstitial water of MCsome, the isomerization of FpC_6Azobenzene MCsome were analyzed using UV-Vis spectroscopy. The sample was irradiated with long wave UV (365 nm) for 30 seconds and 60 seconds to induce the isomerization.

The instrument used for these experiments was the ThermoScientific Genesys 150 UV-Vis spectrophotometer. The wavelength range of UV absorbance of 200 nm to 600 nm was used, and a quartz cell with a light path of 1 cm was used.

3. Temperature-dependent Constructional Water for Self-Assembled Vesicular Membranes

This chapter discusses the temperature-dependent interstitial water of FpR MCsome in terms of its contribution to the integrity of the colloids, confinement of the non-polar groups and the energy dissipation. FpR (R = C_6Pyrene, C_6, C_6Azobenzene) MCsome were prepared at 25 °C by adding water into the THF solution of the FpR molecules followed by a dialysis against water to remove THF. The resultant colloids in water were aged at various temperatures (6 °C, 25 °C, 50 °C and 70 °C) for 24 hours and 5 days in some cases. The temperature-dependent swelling behavior, fluorescence, and isomerization of the azobenzene group were characterized by using DLS, fluorescence and UV-Vis spectroscopies. The resultant data are analyzed and discussed.

3.1 The temperature-dependent integrity of MCsome.

As shown in Figure 17a, the D_h is 105 nm, 108 nm, 109 nm, 109 nm, and 114 nm for the FpC_6Pyrene MCsome after aging at 6 °C, 25 °C, 40 °C, 50 °C, and 70 °C for 24 hours, respectively. This result indicates that the colloids slightly swell at a higher temperature. We have previously reported that the hydrogen bonding structure of the interstitial water for FpC_6Pyrene MCsome has a tetrahedral order, which contributes to the structural integrity of the vesicular membrane.[10] It is known that hydrogen bonding structure of water is sensitive to temperature,[32,33] and the number of hydrogen bonds per water molecule and their strengths decrease as temperature increases.[34,35] Therefore, the swelling behavior, particularly at 70 °C, is attributed to the destruction of the interstitial water.

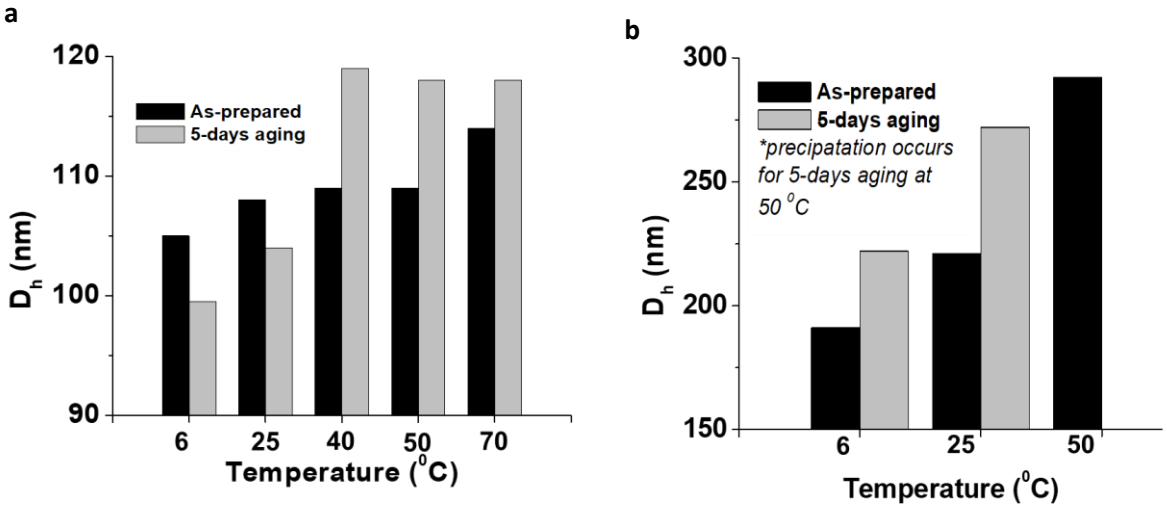

Figure 17: The analysis of D_h for a) FpC_6Pyrene and b) FpC_6 MCsome as prepared and after 5 days of aging at their respective temperatures.

It is reported that the hydrophobicity of the R group determines the structure order of the interstitial water.[10] The less hydrophobic C_6, as compared with C_6Pyrene, induces weaker and less ordered hydrogen bonds for the interstitial water that undergoes further destruction upon aging resulting in swelling.[10] As shown in Figure 17b, the temperature-dependent swelling is more obvious for FpC_6 MCsome, which can be explained by the less ordered interstitial water that is easier to be de-structured at a higher temperature. Upon aging for 5 days at 6 $^\circ$C and 25 $^\circ$C, FpC_6 MCsome swell by 31 nm and 51 nm in the ΔD_h, respectively (Figure 17b), suggesting that the colloids have a less degree of integrity at higher temperatures. By further increasing temperature (50 $^\circ$C), small amounts of precipitates were observed after 5 days aging (Figure 17b and Table S1), suggesting the loss of the integrity of the colloids.

For the FpC_6Pyrene MCsome with well-structured interstitial water,[10] the temperature-dependent 5 days aging behavior is interesting. As shown in Figure 17a, at higher temperatures (40 $^\circ$C, 50 $^\circ$C, and 70 $^\circ$C), a small degree of swelling is observed after 5 days aging and the sample aged at 70 $^\circ$C became less uniform in size as indicated by the high PDI (Table S1). This result is probably due to the less structured water at high temperatures, [34,35] which influences the structural integrity of the MCsome. In contrast, the FpC_6Pyrene MCsome shrinks in size by a ΔD_h of - 6 nm and – 4 nm after aging at 6 $^\circ$C and 25 $^\circ$C for 5 days,

respectively. The decrease in D_h over 5 days at the lower temperatures seems to suggest the lower temperature helps to restructure the interstitial water at 6 °C, which increase the binding force for the building blocks of the MCsome. This explanation can be verified by using Raman spectroscopy, ^{1}H NMR and low field NMR.

We further explored how the interstitial water was affected by cooling the FpC_6Pyrene MCsome from a higher temperature (40 °C, 50 °C, and 70 °C) to either 6 °C or 25 °C. As seen in Figure 18, after cooling from various temperatures (40 °C, 50 °C, and 70 °C) and subsequently aging at 6 °C or 25 °C for 24 hours, the D_h of the colloids decreases. This decrease in the D_h is attributed to the thermal contraction of the less structured interstitial water upon the cooling. This explanation is reasonable, because water molecules tend to have a decrease in the rotational and translational movement at a lower temperature,[32,33] which reduces the volume. It is noted that the D_h is much smaller (113 nm) for the colloids cooled from 70 °C to 6 °C, as compared to those cooling from 40 °C or 50 °C (127 nm or 122 nm, respectively) (Figure 17a). This behavior probably is related to the water structure at various temperatures before the cooling. The MCsome aged at a higher temperature (70 °C) has less structured interstitial water, which was trapped upon cooling. The reconstruction of this trapped water confined within the membrane may not be fast, so this water shrinks at a larger degree because of thermal contraction. The cooling to 6 °C shrinks the colloids. To understand the effect of the freezing temperature (6 °C), we experimented to cool the colloids to room temperature (25 °C). As shown in Table 5, the D_h is similar for the colloids at 25 °C cooled from 40 °C, 50 °C, and 70 °C. It is understandable because, as compared to lower temperatures (6 °C), the room temperature (25 °C) is not able to reconstruct the interstitial water, so all the colloids at this temperature would have similar interstitial water in terms of structure and dynamics.

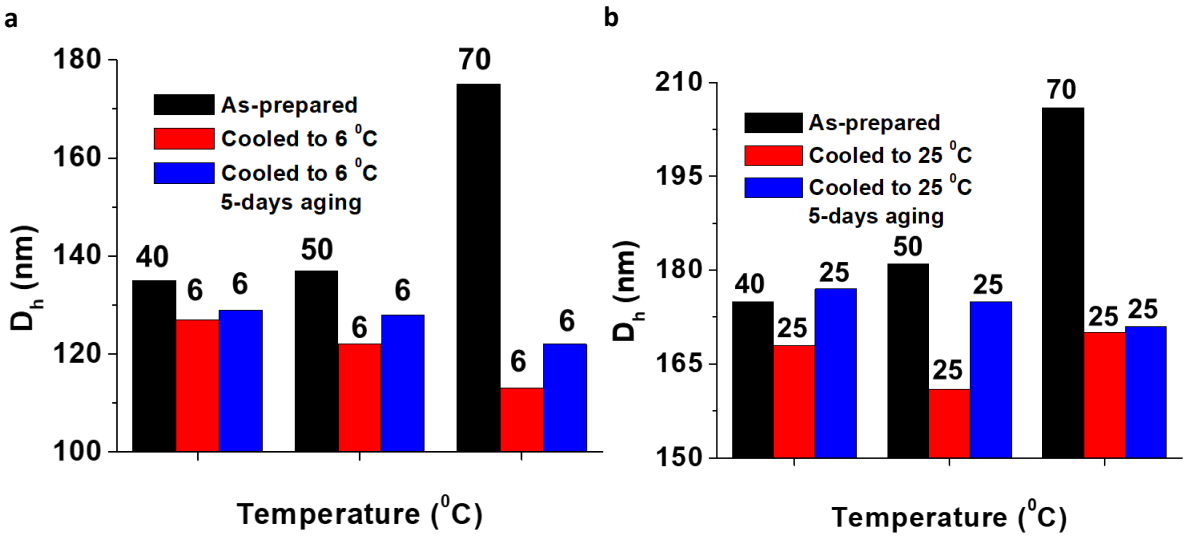

Figure 18: The analysis of D_h for FpC$_6$Pyrene MCsome cooled from various temperatures to a) 6 °C and b) 25 °C.

The effect of aging on the swelling was investigated. After aging at 6 °C for 5 days, the colloids cooling from 70 °C swells from 113 nm to 122 nm. However, the colloids cooled from 50 °C and 40 °C swells less (Figure 18a). It is possible that the interstitial water of the MCsome at a higher temperature, e.g.,70 °C, is less structured, which is quickly frozen upon cooling at 6 °C. The tendency to reconstruct the interstitial water during aging at 6 °C expands the volume, which explains the swelling. Due to the significant swelling behaviour of the colloids after aging from 70 °C to 6 °C, it may suggest that the reconstructing process could be much longer than 5 days and would be interesting to further study. For the colloids cooled from 40 °C, they barely swell. The interstitial water structure at 40 °C may not be significantly disrupted, which allowed them to be restructured easily during the cooling process. Therefore, the resultant ordered interstitial water is relatively stable and does not change in volume. The swelling is also observed for the colloids cooling from various temperatures to 25 °C after 5 days aging (Figure 18b), but the degree of the swelling is independent from the temperatures before cooling. This could be explained since 25 °C is not cold enough to freeze the interstitial water molecules. Therefore, the interstitial water for all colloids cooled from different temperatures to 25 °C are similar in mobility. The relatively higher mobility at 25 °C, relative to 6 °C, accounts for the swelling. Overall, the temperature from which to cool

and the final cooling temperature are important. At high temperatures (> 50 °C), the interstitial water is less structured, which can be frozen by cooling to 6 °C, but not 25 °C. The frozen interstitial water at 6 °C may undergo reconstruction, but it will probably take a longer time of cooling, which is an interesting topic for further research.

As discussed above (Figure 18a), the colloids cooled from higher temperature (>50 °C) to 6 °C freezes the interstitial water and the reconstruction of the water takes time. However, cooling from 40 °C is accompanied with the reconstruction of the interstitial water. It suggests that the interstitial water structure can be reversibly restructured quickly by varying the temperatures below 40 °C. One example is shown in Table 3, where the size of the MCsome can be changed reversibly between 25 °C and 6 °C. As seen in the table, the size of the colloids at 25 °C is 210 nm. Upon cooling to 6 °C, the size of the colloids shrinks to 182 nm. Reheating the colloids back to 25 °C swells the size back to 210 nm. This temperature-dependent reversibility can be attributed to the changes in the interstitial water structure as previously discussed. This demonstrates that the size of the MCsome can be quickly reversible by varying the temperature below 40 °C, which can be attributed to the possible reversible changes in the interstitial water structure.

Table 3: The analysis of D_h and PDI, and the calculation of I_1:I_3 ratio of FpC_6Pyrene MCsome subjected to alternating temperatures.

Temperature	D_h / PDI / I_1:I_3 ratio
25°C	210 nm / 0.08 / 1.64
25°C → 6°C	182 nm / 0.03 / 1.50
6°C → 25°C	210 nm / 0.06 / 1.74

3.2 The temperature-dependent polarity and cohesive energy of the interstitial water.

The contribution of the interstitial water to the temperature-dependent colloidal behavior was further investigated by using FpC_6Pyrene and FpC_6Azobenzene MCsome, in which the pyrene and azobenzene groups are surrounded by the interstitial water.[10,16] The fluorescence of the pyrene groups [37,38] and the UV-light stimulated *trans*-to-*cis* isomerization of the azobenzene groups were used to probe the temperature-dependent polarity,[39] and the cohesive energy of the interstitial water,[16] respectively.

The polarity of the interstitial water surrounding the pyrene groups within the vesicular membrane is expressed by the I_1:I_3 ratio as shown in Figure 19. As seen in the table, the I_1:I_3 ratio is 1.58, 1.80, 2.02, 2.05, and 2.08 for the FpC_6Pyrene MCsome after aging for 24 hours at 6 ˚C, 25 ˚C, 50 ˚C, and 70 ˚C respectively. It suggests that the polarity of the interstitial water increases with raising the temperature. The lower polarity at 6 ˚C, even after aging for 5 days, suggests that the interstitial water has well-structured tetrahedral order,[36] which will be verified by Raman spectroscopy. For other MCsome aging at temperatures larger than 6 ˚C, the increase in the polarity, as indicated by the I_1:I_3 ratio, is detected after 5 days aging (Figure19). This analysis indicates that the higher temperature and longer time aging increases the polarity, which can be attributed to destruction of the interstitial water. As a result, the interstitial water has faster dynamics and less hydrogen bonding,[35,36] which is a possible reason for the observed swelling (Figure 17a).

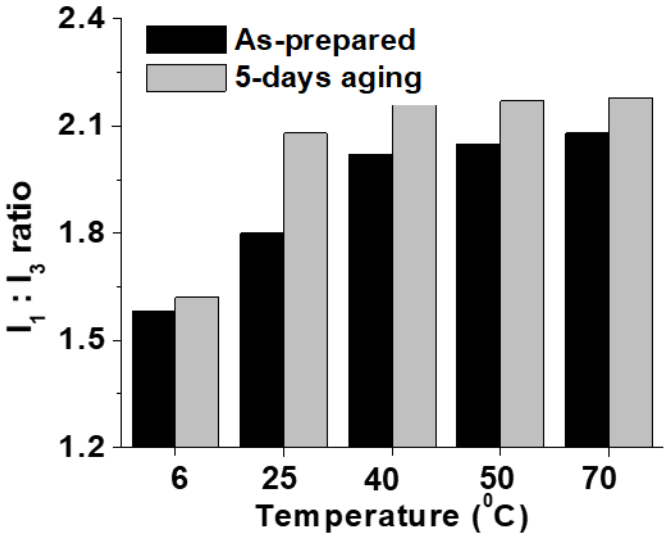

Figure 19: The analysis of the interstitial water polarity (I_1:I_3 ratio) for FpC_6Pyrene MCsome at different temperatures.

We investigated the effect of the cooling on the polarity of interstitial water. As seen in Figure 20a, when the sample was cooled from 40 ˚C to 6 ˚C, the polarity decreases as the I_1:I_3 ratio decreases from 1.81 to 1.63 (after aging 24 hours) and 1.60 (after aging 5 days). However, there is a slight increase in the polarity when the colloids are cooled from higher temperature (50 ˚C and 70 ˚C) to 6 ˚C, which are indicated by a

slightly increase (from 2.01 to 2.06 and 2.10 to 2.16, respectively) in the I_1:I_3 ratios (Figure 20a). It is attributed to the less structured water at a higher temperature that is frozen by the fast cooling to 6 °C. After 5 days aging, an obvious decrease in the I_1:I_3 ratio (from 2.06 to 1.80) is observed for the colloids cooled from 50 °C to 6 °C and only a slight decrease (from 2.16 to 2.10) is noted for the colloids cooled from 70 °C to 6 °C. It may suggest that the former colloids (50 °C) have a higher tendency to restructure the water at 6 °C. It is possibly attributed to the temperature-dependent structure of the interstitial water before cooling. The interstitial water structure at 50 °C is less broken as compared to that at 70 °C. Therefore, it is easier for the reconstruction of the interstitial water after cooling from 50 °C to 6 °C in comparison to the cooling from 70 °C to 6 °C. Therefore, we learned that the reconstruction of the nano-confined interstitial water at 6 °C would be difficult if the colloids experienced a higher temperature treatment (70 °C). A longer aging time at 6 °C may gradually re-structure the water. This hypothesis will be examined as a future work. We also investigated the effect of cooling to room temperature on the polarity of interstitial water. As seen in Figure 20b, the I_1:I_3 ratio slightly decreases and remains similar for all samples, even after 5 days of aging at room temperatures. This suggests that interstitial water structure and dynamics are similar between all samples after cooling. This could be explained since 25 °C is not cold enough to reconstruct the interstitial water, thus resulting in all samples having similar less structured interstitial water. Therefore, we also learned that the cooling temperature is important in allowing for the reconstruction of the interstitial water to occur.

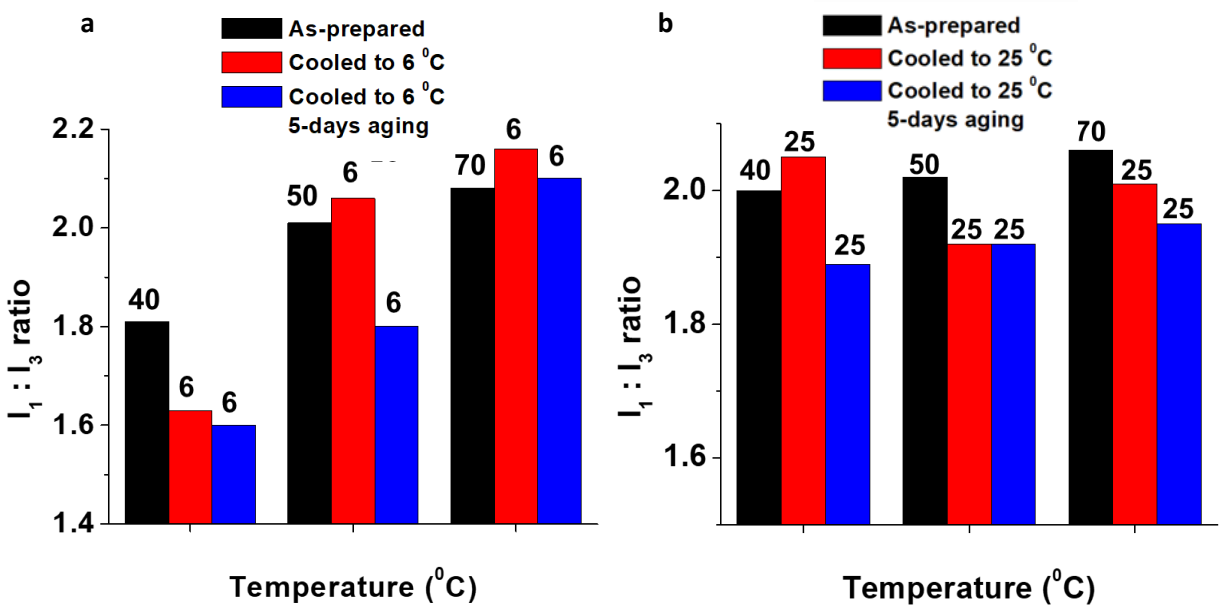

Figure 20: The analysis of the interstitial water polarity (I_1: I_3 ratio) for FpC_6Pyrene MCsome cooled from various temperatures to a) 6 °C and b) 25 °C.

It is worth noting that the D_h and I_1:I_3 for the samples prepared at various temperatures are different in Table S2 and S3, although they are prepared using the same procedures. For example, the I_1:I_3 ratio at 40 °C is 1.81 and 2.00 in Table S2 and S3, respectively. This difference is caused by the high sensitivity of the self-assembly to the preparation conditions as we have discussed in Chapter 2. Nevertheless, the trend for the temperature influenced interstitial water is the same regardless of the initial D_h and I_1:I_3 ratio.

As discussed previously, it is noted that the changes in the interstitial water structure can be reversible at temperatures below 40 °C. Therefore, the reversibility of the polarity of MCsome between 25 °C and 6 °C was also calculated using the I_1:I_3 ratio as seen in Table 6. As seen in the table, the initial I_1:I_3 ratio at 25 °C was calculated to be at 1.64. When the MCsome was cooled from 25 °C to 6 °C, the I_1:I_3 ratio dropped to 1.50. When the MCsome was heated from 6 °C back to 25 °C, the I_1:I_3 ratio increased to 1.74. These results are possibly due to the response of the interstitial water structure to temperature as previously stated. It further supports that the interstitial water structure can be reversible quickly at temperatures below 40 °C.

The temperature-dependent I_1:I_3 ratio of pyrene molecules in water was investigated to compare with the pyrene groups confined within the interstitial water, which will help us to understand the nano-confinement effects. The solution was prepared by adding excess pyrene (3 g) into MiliQ water (10 mL) and the resultant solutions were continuously stirred for 3 days. Afterwards, the solution was centrifuged, and the supernatant was collected. This water solution was then aged at various temperatures (6 $^{\circ}$C, 25 $^{\circ}$C and 50 $^{\circ}$C) for 24 hours. The solutions were removed from the aging conditions and was immediately analyzed by fluorescence spectroscopy. The I_1:I_3 ratio was then calculated from the spectra and displayed in Table 7. As seen in the table, the I_1:I_3 ratio decreases with increasing temperature. This result is consistent with the literature reported,[31,37] and can be explained by the parameters determining the polarity of water: including (1) the hydrogen bond donor (α), (2) hydrogen bond acceptor (β) capability and (3) dipolarity/polarizability (π*) of water known as the Kamlet-Taft solvent parameters.[31,40] The third parameter is the most sensitive to temperatures, and it was found that the π* of water decreases with increasing temperature.[31,40,41] This explains the decrease in I_1:I_3 ratio with increasing temperature for pyrene molecules in bulk water.[31,37]

Table 4: Calculation of I_1:I_3 ratio for pyrene in water.

Temperature of pyrene in water solution*	I_1:I_3 ratio of pyrene in water
6 °C	2.32
25 °C	2.06
50 °C	1.60

*Pyrene in water solution were prepared by mixing pyrene in water for 3 days. The solution was then centrifuged, and the supernatant was collected and aged at their respective temperature for 24 hours.

The interstitial water is different with bulk water, which is well-structured with ice-like tetrahedral order of hydrogen bonds and thus has a lower polarity.[39] In addition, the nano-confinement by the membrane restricts the rotational and translational dynamics of water, which also reduces the polarity.[36] Although π* would be larger by decreasing temperature,[31] the tendency for an increase in the tetrahedral order at cold temperatures (6 $^{\circ}$C) may become a major factor influencing the polarity. This explains that the interstitial water, unlike bulk water, has a lower polarity at a colder temperature as aforementioned. The

difference in the temperature dependent-polarity of bulk and the interstitial water indicates that the nano-confinement influences the water structures. This effect can be verified by using Raman spectroscopy to directly analyze water structures. It is also possible to probe this effect by measuring the variation of water cohesive energy (related to the water structures) under various conditions, e.g. in response to temperature.

The temperature-dependent cohesive energy of the interstitial water was investigated by using FpC_6Azobenzene MCsome, whose membrane contains azobenzene groups. The UV-stimulated *trans*-to-*cis* isomerization rate [42-44] would be dependent on the confinement force of the interstitial water, which is an indicator for the cohesive energy.[6,16] The FpC_6Azobenzene colloids were prepared at 25 °C and aged at various temperatures for 24 hours. The resultant colloids were then irradiated by using UV light (365 nm) for 30 and 60 seconds to stimulate the isomerization. The UV-Vis spectra for the solutions irradiated for various times are recorded and displayed in Figure 21. As shown in the figure, the spectra for the solutions prepared at 6 °C, 25 °C, and 50 °C are the same and overlapped, suggesting that the temperature does not trigger a detectible isomerization. Upon the irradiation by the UV light, the absorption at 355 nm decreases in the intensity indicating that the isomerization is trigged. This decreasing in the absorption at 355 nm is faster for the sample prepared at 50 °C, which suggests that the restriction force for the isomerization is weaker. Therefore, a higher temperature (50 °C) reduces the cohesive energy of the interstitial water, which is in line with the destruction of the tetrahedral order as indicated by the increase in the polarity (Figure 19). This temperature-dependent cohesive energy also explains the swelling behavior of MCsome at a high temperature (Figure 17a).

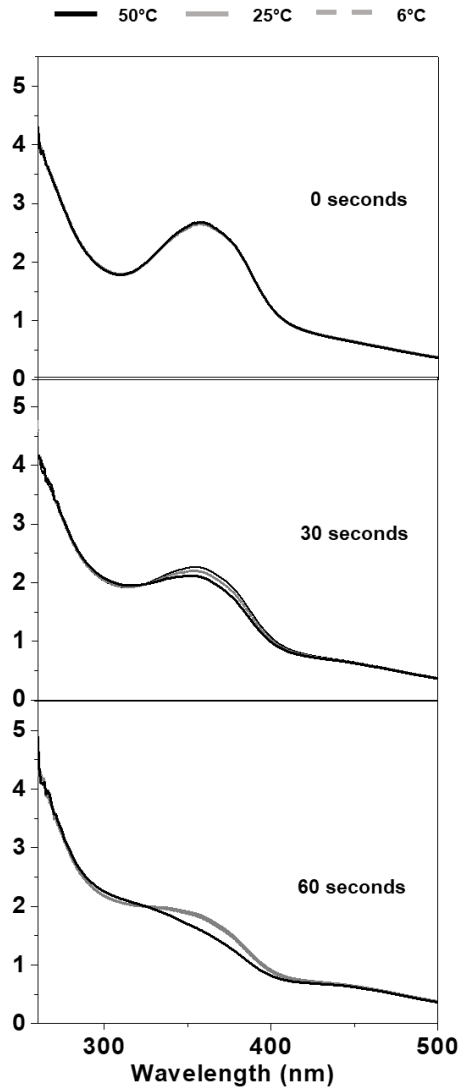

Figure 21: Time-dependent UV-Vis spectra (0, 30, 60 seconds) for FpC_6Azobenzene MCsome prepared at various temperatures (6 ˚C, 25 ˚C, and 50 ˚C).

3.3 Energy dissipation by the interstitial water.

The temperature-dependent fluorescence intensity of FpC_6Pyrene MCsome in water was further investigated. Figure 22 illustrates the fluorescence spectra for the colloids at various temperatures, from which it is obvious that the fluorescence intensity decreases with decreasing temperature. It suggests that the colloids have a temperature-dependent energy dissipation. The tetrahedral structure of the interstitial

water in response to the temperature is a possible reason. The degree of the tetrahedral order of the interstitial water increases as the temperature decreases, so the weaker fluorescence intensity at a lower temperature is probably caused by the tetrahedral order that dissipates the energy. The structured water has oriental constraints in the water molecules,[36] which have stronger hydrogen bonds between the water molecules and dangling OH groups interacting directly with the pyrene groups.[10]

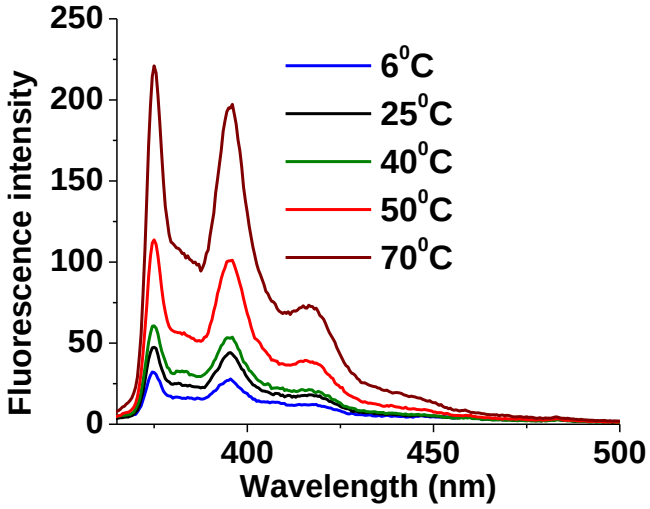

Figure 22: Fluorescence spectra of FpC_6Pyrene MCsome in water at different temperatures.

Figure 20 illustrates the fluorescence spectra for the FpC_6Pyrene MCsome after aging at various temperatures for 5 days. As probed by pyrene groups, for the 5 days aging at 6 ˚C, I_1:I_3 ratio remains low from 1.58 to 1.62 (Figure 20a). This subtle change in the polarity may be due to the experimental error. However, the fluorescence intensity obviously drops after the aging, which suggests an increase in the energy dissipation. This result implies that the aging at 6 ˚C increases the water structure and the fluorescence intensity measurement is more sensitive to this change (Figure 23a). In contrast, the fluorescence intensity is enhanced upon aging at 25 ˚C (Figure 23b), suggesting a decrease in the energy dissipation. This is attributed to the destruction of the interstitial water after aging at room temperature that is not able to integrate the water structure.[10] When the aging temperature is higher (40 ˚C, 50 ˚C, 70 ˚C), the increase in the fluorescence intensity is more obvious and proportional to the aging temperature (Figure 23c-e). Therefore, the water structure plays an important role in the dissipation energy.

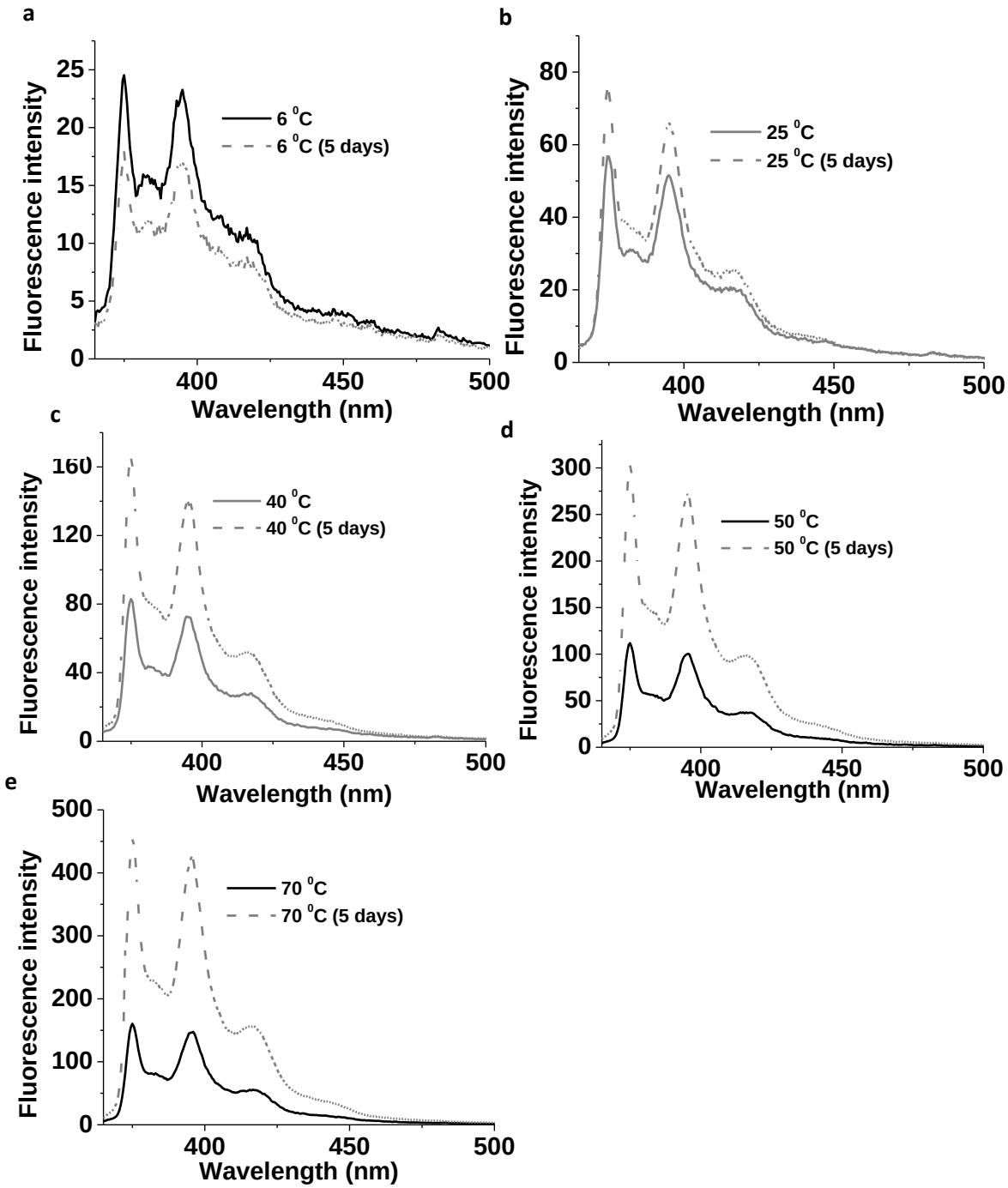

Figure 23: Fluorescence spectra of FpC_6Pyrene MCsome in water before and after aging at a) 6 °C, b) 25 °C, c) 50 °C, and d) 70 °C for 5 days.

The heating of the MCsome is a parameter influencing the structure of the interstitial water, which has been probed by the I_1:I_3 ratio as discussed previously. We intend to verify this parameter by taking

advantage of the dependence of the energy dissipation on the structure of interstitial water after cooling the colloids. To verify the role of water in the energy dissipation, the cooling effect is investigated. The fluorescence spectra for the colloids at various temperatures (40 °C, 50 °C and 70 °C) were recorded first, then the solutions were cooled to 6 °C and subsequently aged at this temperature for 24 h and 5 days before recording the fluorescence spectra. All the spectra are displayed in Figure 24. As shown in the figure, the cooling reduces the fluorescence intensities, which is explained by the enhancement in energy dissipation due to the freezing of the water structure at 6 °C and is consistent with the above discussion. The fluorescence intensity variation after aging at 6 °C for 5 days is dependent on the sample temperature before cooling. There is barely change for the sample cooled from 40 °C (Figure 24a), but an obvious decrease in the intensity for the samples cooled from 50 °C and 70 °C (Figure 24b and c, respectively) is noted. As we have discussed above, the interstitial water cooled from 40 °C to 6 °C can restructure the interstitial water quickly, so the interstitial water remains stable upon the aging and do not vary its ability to dissipate energy significantly. However, cooling from higher temperatures may only freeze the de-structured water. The reconstruction of the water at 6 °C over time will increase the dissipation energy, which explains the decrease in the fluorescence intensity. This reconstruction is slow and may related to the nano-confinement, which be further examined by performing kinetic studies.

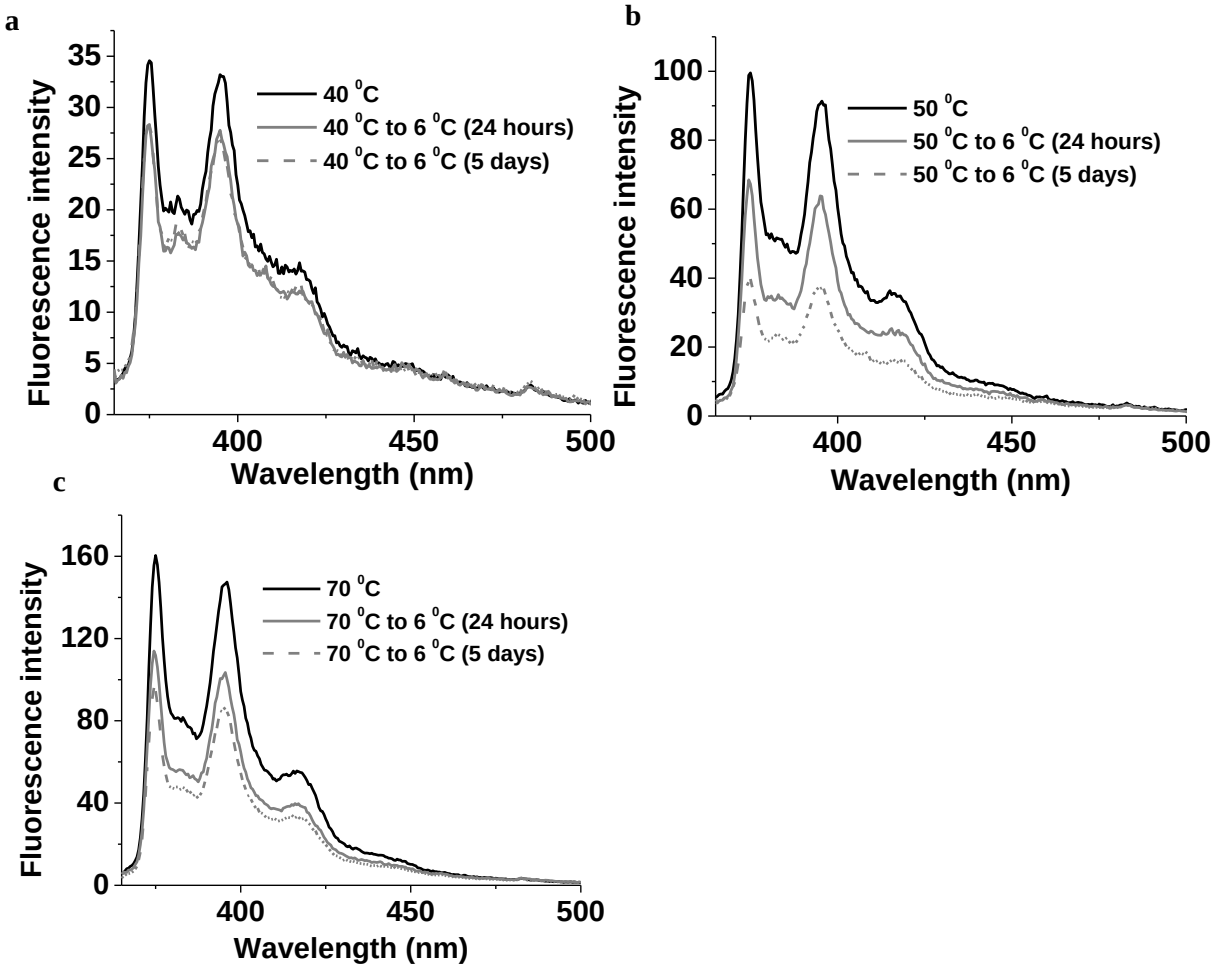

Figure 24: Fluorescence spectra of a) FpC_6Pyrene MCsome in water at 40 °C and cooling to 6 °C, b) FpC_6Pyrene MCsome in water at 50 °C and cooling to 6 °C, and c) FpC_6Pyrene MCsome in water at 70 °C and cooling to 6 °C.

To further examine the effect of the cooling temperature, the control experiments by cooling to 25 °C were performed. The similar fluorescence behavior in response to cooling to 25 °C is observed (Figure 25), but the variation in fluorescence is much weaker compared to the solution cooling to 6 °C (Figure 24). This is further supported by the slight decrease in polarity as indicated by the change in I_1:I_3 ratio (Figure 20a). It suggests that a colder temperature (6 °C) is needed to help encourage the energy dissipation due to an increase in tetrahedral order over time.

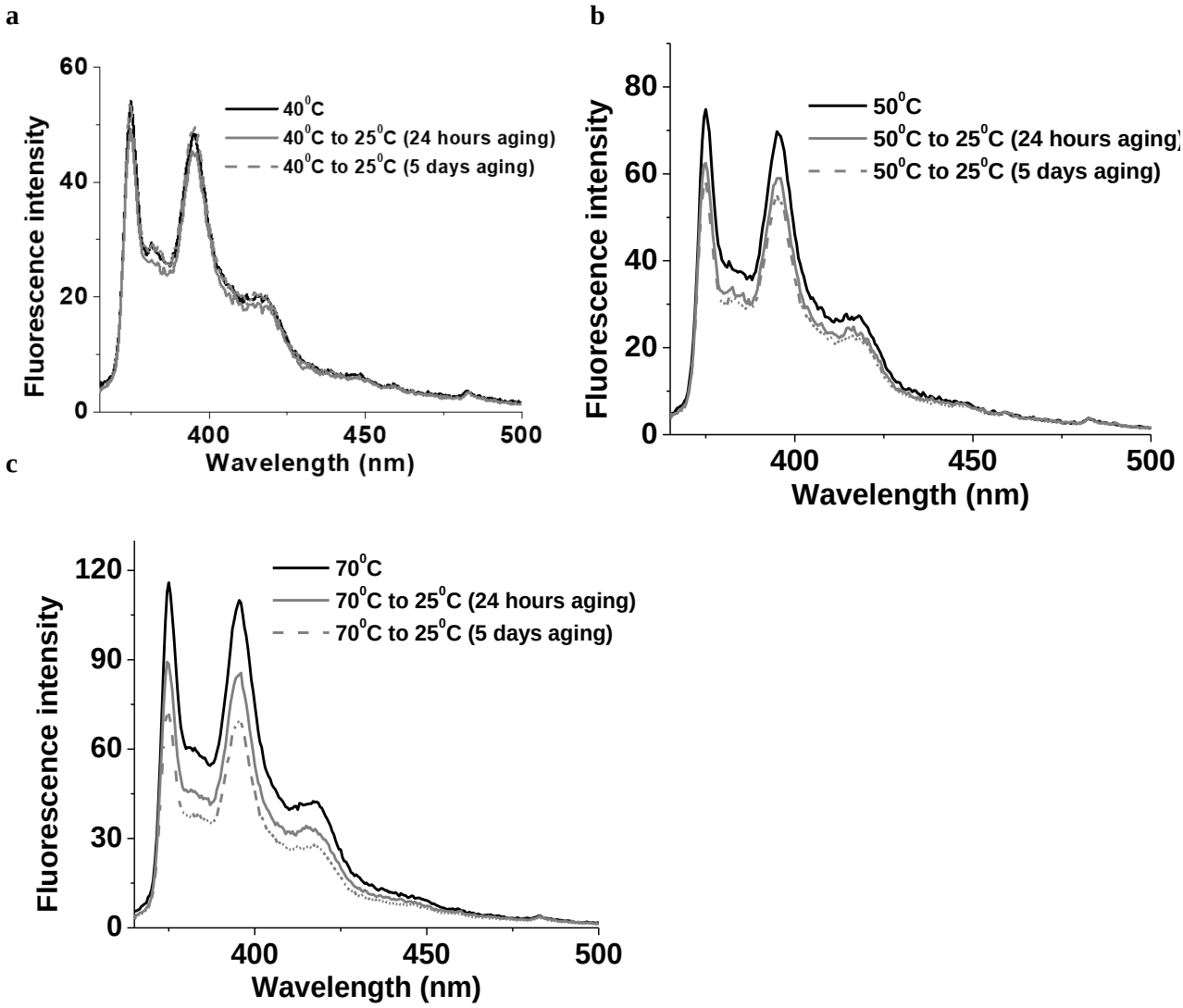

Figure 25: Fluorescence spectra of a) FpC_6Pyrene MCsome in water at 40 ˚C and cooling to 25 ˚C, b) FpC_6Pyrene MCsome in water at 50 ˚C and cooling to 25 ˚C, and c) FpC_6Pyrene MCsome in water at 70 ˚C and cooling to 25 ˚C.

As discussed previously, it is noted that the changes in the interstitial water structure can be reversible between 25 °C and 6 °C. Therefore, fluorescence analysis was done on the resultant MCsome to investigate the possible reversibility of energy dissipation as seen in Figure 26. As seen in the figure, when the temperature increases to 25 °C, the fluorescence intensity increases and when the temperature decreases to 6°C, the fluorescence intensity decreases. This is in response to the change in energy dissipation, which

is dependent on the interstitial water structure as previously discussed. This indicates that the energy dissipation of the interstitial water is also quickly reversible at temperatures below 40 °C.

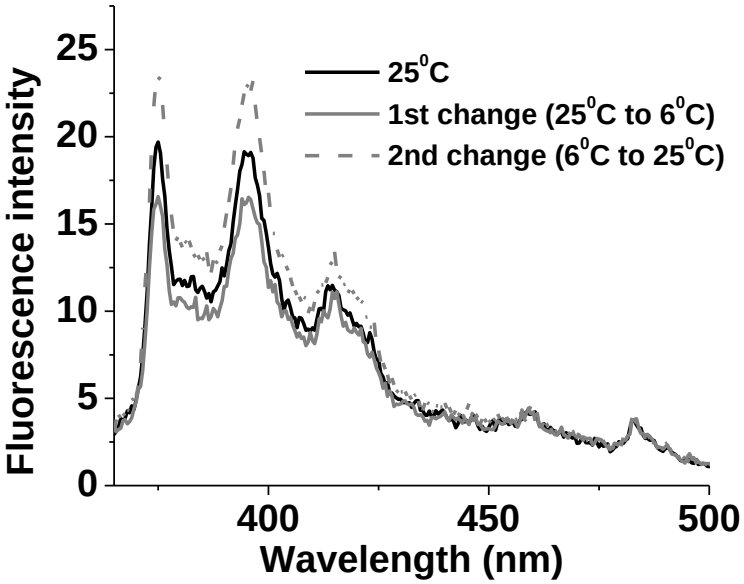

Figure 26: Fluorescence spectra of FpC_6Pyrene MCsome in water subjected to alternating temperatures. The temperature of FpC_6Pyrene MCsome were changed between 6°C and 25°C.

The temperature-dependent fluorescence intensity of pyrene in water (Figure 27) is compared with that for the pyrene group confined within the interstitial water (Figure 22). The same behavior is found as the fluorescence intensity decreases as the solutions are cooled. The difference is that the intensity drops more significantly for the pyrene groups confined by the interstitial water (Figure 22), which is attributed to the tetrahedral order of the water within the membrane. The nano-confined interstitial water could be more structured with strong hydrogen bonds in comparison to the hydration water of pyrene molecules. This can result in a stronger energy dissipation for the interstitial water in comparison to the hydration water of pyrene molecules.

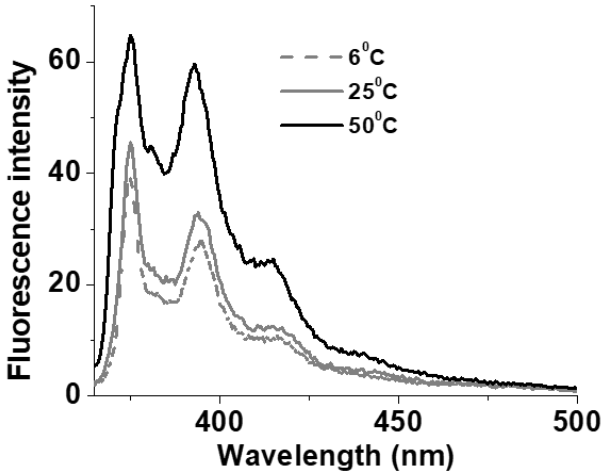

Figure 27: Fluorescence spectra of pyrene in water at 6 °C, 25 °C, and 50 °C.

Energy dissipation by water media has been studied. It has been reported that the energy dissipation of protein hydration water was important in the investigation of protein dynamics using Brillouin neutron spectroscopy.[45] Brillouin neutron spectroscopy measures the dispersion of the neutrons based on a given material at a given temperature.[45] As investigated by Orecchini et al., the dispersion of the neutrons was based on the changes in the local structure of the hydration water within the protein's surface, in which a more structured hydration water can disperse the neutrons much more.[45] With this information, the disordering effect based on the dynamics of ribonuclease A (RNase) was found to be induced by changes within the hydration water structure on the protein's surface.[45] Therefore, the structured interstitial water within MCsome may play a role in the energy dissipation to dim the fluorescence, thus making fluorescence spectroscopy another technique that can be used to measure energy dissipation.

4. Conclusion

In conclusion, the preparation of FpC_6Pyrene MCsome was investigated and several factors that influence the resultant MCsome were determined, which include water quality, the order of mixing water and the THF solution of FpC_6Pyrene, and the rate of water addition. The temperature effect on the interstitial water of MCsome was also investigated. It was found that warmer temperatures induce the swelling while colder temperatures shrink the MCsome. This behaviour is attributed to the change in interstitial water structure, which was further analyzed using fluorescence spectroscopy and UV-Vis spectroscopy to analyze changes in polarity and cohesive energy. Increasing the temperature was found to increase the polarity and decrease the cohesive energy, while decreasing the temperature was found to decrease the polarity and increase the cohesive energy of the interstitial water. This behaviour is also attributed to the change in the interstitial water structure and dynamics where increasing temperature breaks the interstitial water structure. The changes in the temperature-dependent interstitial water structure were also detected by the energy dissipation of fluorescence *via* the fluorescence emission of FpC_6Pyrene. The increase in interstitial water structure with colder temperatures allows for the energy to be highly dissipated. With this knowledge, it was found that the cooling temperature of the colloids is important in the reconstruction of the interstitial water. Colder temperatures are found to reconstruct the interstitial water more quickly unlike cooling to room temperature. Furthermore, the changes in the temperature-dependent interstitial water are reversible when the temperature is below 40 °C since their interstitial water structure can be reconstructed more quickly. Overall, this investigation highlights the importance of water in the self-assembly of FpR molecules. This class of materials can be used to obtain knowledge for the design of novel colloids and understanding biological systems.

5. Future work

Although the preparation parameters of FpR MCsome was investigated and several factors were determined, a more in-depth investigation is needed to fully understand how these factors are influencing MCsome. The calculation of the I_1:I_3 ratio and subsequent investigation in the energy dissipation properties of FpR MCsome prepared from water with various pH can help us understand the significance of water quality in the preparation step.

To understand the FpR as kinetic assemblies, the rate of water addition as a factor influencing the resultant MCsome will also be further investigated by varying the rate of water addition into the THF solution of FpR. This could give an insight on the role of water in kinetic assemblies as the assemblies vary depending on the rate of water addition as previously discussed. Another investigation that can be also used to study FpR as kinetic assemblies is the order of mixing water and the THF solution of FpC_6Pyrene.

The temperature-dependent interstitial water was probed by the pyrene group of FpC_6Pyrene, which gave insight on the possible changes in water structure and dynamics based on changing polarity *via* I_1:I_3 ratio. However, further experiments are needed to confirm the temperature-dependent change in interstitial water structure and dynamics. Raman spectroscopy and low-field NMR can be used to investigate the temperature-dependent change in interstitial water structure by analyzing the change in hydrogen bonding and interaction. To study the temperature-dependent interstitial water dynamics, time-dependent IR anisotropy can be used to analyze the orientational relaxation of the interstitial water, which is a technique that has been previously used for research on nano-confined water.[26,27] The effect of cooling the MCsome from high temperatures suggests gradual changes within the interstitial water over time. However, a longer cooling time would be needed to further investigate the reconstruction of the interstitial water.

6. References

1. Xing, P.; Sun, T.; Hao, A. Vesicles From Supramolecular Amphiphiles. *RSC Advances* 2013, *3* (47), 24776.
2. Lombardo, D.; Kiselev, M.; Magazù, S.; Calandra, P. Amphiphiles Self-Assembly: Basic Concepts And Future Perspectives Of Supramolecular Approaches. *Advances in Condensed Matter Physics* 2015, *2015*, 1-22.
3. Zakharova, L.; Pashirova, T.; Doktorovova, S.; Fernandes, A.; Sanchez-Lopez, E.; Silva, A.; Souto, S.; Souto, E. Cationic Surfactants: Self-Assembly, Structure-Activity Correlation And Their Biological Applications. *International Journal of Molecular Sciences* 2019, *20* (22), 5534.
4. Murshid, N.; Wang, X. Iron-Carbonyl Aqueous Vesicles (Mcsomes) By Hydration Of [Fe(CO){CO(CH2)5CH3}(Cp)(Pph3)] (Fpc6): Highly Integrated Colloids With Aggregation-Induced Self-Enhanced IR Absorption (AI-SEIRA). *Chemistry - A European Journal* 2015, *21* (52), 19223-19230.
5. Murshid, N.; Wang, X. Hydrophobic Effect Of Alkyl Groups Stabilizing Self-Assembled Colloids In Water. *The Journal of Physical Chemistry B* 2017, *121* (25), 6280-6285.
6. Liu, D.; Wang, X. Hierarchical Self-Assembly Induced By Dilution-Enhanced Hydrophobic Hydration. *Chemistry - A European Journal* 2018, *24* (26), 6737-6741.
7. Shi, S.; Liu, D.; Wang, X. The Effect Of Solution Conditions On The Driving Forces For Self-Assembly Of A Pyrene Molecule. *Chemistry - A European Journal* 2017, *23* (41), 9736-9740.
8. Murshid, N.; Yuyama, K.; Wu, S.; Wu, K.; Masuhara, H.; Wang, C.; Wang, X. Highly-Integrated, Laser Manipulable Aqueous Metal Carbonyl Vesicles (Mcsomes) With Aggregation-Induced Emission (AIE) And Aggregation-Enhanced IR Absorption (AEIRA). *Journal of Materials Chemistry C* 2016, *4* (23), 5231-5240.

9. Foucher, D.; Honeyman, C.; Nelson, J.; Tang, B.; Manners, I. Organometallic Ferrocenyl Polymers Displaying Tunable Cooperative Interactions Between Transition Metal Centers. *Angewandte Chemie International Edition in English* 1993, *32* (12), 1709-1711.
10. Yang, Y.; Chen, C.; Liu, D.; Raj, A.; Hamaguchi, H.; Qiu, H.; Lin, Y.; Wang, C.; Wang, X. Vesicular Membrane With Structured Interstitial Water. *The Journal of Physical Chemistry B* 2020, *124* (41), 9239-9245.
11. Okajima, H.; Ando, M.; Hamaguchi, H. Formation Of "Nano-Ice" And Density Maximum Anomaly Of Water. *Bulletin of the Chemical Society of Japan* 2018, *91* (6), 991-997.
12. Davis, J.; Gierszal, K.; Wang, P.; Ben-Amotz, D. Water Structural Transformation At Molecular Hydrophobic Interfaces. *Nature* 2012, *491* (7425), 582-585.
13. Perera, P.; Fega, K.; Lawrence, C.; Sundstrom, E.; Tomlinson-Phillips, J.; Ben-Amotz, D. Observation Of Water Dangling OH Bonds Around Dissolved Nonpolar Groups. *Proceedings of the National Academy of Sciences* 2009, *106* (30), 12230-12234.
14. Grdadolnik, J.; Merzel, F.; Avbelj, F. Origin Of Hydrophobicity And Enhanced Water Hydrogen Bond Strength Near Purely Hydrophobic Solutes. *Proceedings of the National Academy of Sciences* 2016, *114* (2), 322-327.
15. Merzel, F.; Avbelj, F. Why Do Water Molecules Around Small Hydrophobic Solutes Form Stronger Hydrogen Bonds Than In The Bulk?. *Biochimica et Biophysica Acta (BBA) - General Subjects* 2020, *1864* (4), 129537.
16. Yang, Y.; Zhang, H.; Chen, C.; Liu, D.; Raj, A.; Hamaguchi, H.; Tang, B.; Lin, Y.; Wang, C.; Wang, X. Water-Mediated Through-Space-Conjugation Of Aromatic Groups For Stimuli-Responsive Photoluminescence. *Giant* 2020, *3*, 100028.
17. Scatena, L. Water At Hydrophobic Surfaces: Weak Hydrogen Bonding And Strong Orientation Effects. *Science* 2001, *292* (5518), 908-912.

18. Zichi, D.; Rossky, P. The Equilibrium Solvation Structure For The Solvent-Separated Hydrophobic Bond. *The Journal of Chemical Physics* 1985, *83* (2), 797-808.
19. Hummer, G.; Rasaiah, J.; Noworyta, J. Water Conduction Through The Hydrophobic Channel Of A Carbon Nanotube. *Nature* 2001, *414* (6860), 188-190.
20. Chakraborty, S.; Kumar, H.; Dasgupta, C.; Maiti, P. Confined Water: Structure, Dynamics, And Thermodynamics. *Accounts of Chemical Research* 2017, *50* (9), 2139-2146.
21. Mukherjee, B.; Maiti, P.; Dasgupta, C.; Sood, A. Jump Reorientation Of Water Molecules Confined In Narrow Carbon Nanotubes. *The Journal of Physical Chemistry B* 2009, *113* (30), 10322-10330.
22. Kastelowitz, N.; Molinero, V. Ice–Liquid Oscillations In Nanoconfined Water. *ACS Nano* 2018, *12* (8), 8234-8239.
23. Johnston, J.; Kastelowitz, N.; Molinero, V. Liquid To Quasicrystal Transition In Bilayer Water. *The Journal of Chemical Physics* 2010, *133* (15), 154516.
24. Hanot, S.; Lyonnard, S.; Mossa, S. Water Confined In Self-Assembled Ionic Surfactant Nano-Structures. *Soft Matter* 2015, *11* (12), 2469-2478.
25. Fayer Lab - Nanoscopic Water in Reverse Micelles. https://web.stanford.edu/group/fayer/research_micelle.html (accessed Aug 15, 2021).
26. Moilanen, D.; Levinger, N.; Spry, D.; Fayer, M. Confinement Or The Nature Of The Interface? Dynamics Of Nanoscopic Water. *Journal of the American Chemical Society* 2007, *129* (46), 14311-14318.
27. Moilanen, D.; Fenn, E.; Wong, D.; Fayer, M. Water Dynamics In Large And Small Reverse Micelles: From Two Ensembles To Collective Behavior. *The Journal of Chemical Physics* 2009, *131* (1), 014704.
28. Weik, M. Low-Temperature Behavior Of Water Confined By Biological Macromolecules And Its Relation To Protein Dynamics. *The European Physical Journal E* 2003, *12* (1), 153-158.

29. Sartor, G.; Hallbrucker, A.; Mayer, E. Characterizing The Secondary Hydration Shell On Hydrated Myoglobin, Hemoglobin, And Lysozyme Powders By Its Vitrification Behavior On Cooling And Its Calorimetric Glass-->Liquid Transition And Crystallization Behavior On Reheating. *Biophysical Journal* 1995, *69* (6), 2679-2694.
30. Glushko, V.; Thaler, M.; Karp, C. Pyrene Fluorescence Fine Structure As A Polarity Probe Of Hydrophobic Regions: Behavior In Model Solvents. *Archives of Biochemistry and Biophysics* 1981, *210* (1), 33-42.
31. Trivedi, S.; Malek, N.; Behera, K.; Pandey, S. Temperature-Dependent Solvatochromic Probe Behavior Within Ionic Liquids And (Ionic Liquid + Water) Mixtures. *The Journal of Physical Chemistry B* 2010, *114* (24), 8118-8125.
32. Dougherty, R. Temperature And Pressure Dependence Of Hydrogen Bond Strength: A Perturbation Molecular Orbital Approach. *The Journal of Chemical Physics* 1998, *109* (17), 7372-7378.
33. Smith, J.; Cappa, C.; Wilson, K.; Cohen, R.; Geissler, P.; Saykally, R. Unified Description Of Temperature-Dependent Hydrogen-Bond Rearrangements In Liquid Water. *Proceedings of the National Academy of Sciences* 2005, *102* (40), 14171-14174.
34. Mizan, T.; Savage, P.; Ziff, R. Temperature Dependence Of Hydrogen Bonding In Supercritical Water. *The Journal of Physical Chemistry* 1996, *100* (1), 403-408.
35. Dorsett, H.; Watts, R.; Xantheas, S. Probing Temperature Effects On The Hydrogen Bonding Network Of The Cl-(H2O)2 Cluster. *The Journal of Physical Chemistry A* 1999, *103* (18), 3351-3355.
36. Romero-Vargas Castrillón, S.; Giovambattista, N.; Aksay, I.; Debenedetti, P. Effect Of Surface Polarity On The Structure And Dynamics Of Water In Nanoscale Confinement. *The Journal of Physical Chemistry B* 2009, *113* (5), 1438-1446.
37. Ndou, T.; von Wandruszka, R. Pyrene Fluorescence In Premicellar Solutions: The Effects Of Solvents And Temperature. *Journal of Luminescence* 1990, *46* (1), 33-38.

38. Pietsch, C.; Vollrath, A.; Hoogenboom, R.; Schubert, U. A Fluorescent Thermometer Based On A Pyrene-Labeled Thermoresponsive Polymer. *Sensors* 2010, *10* (9), 7979-7990.
39. Yang, Y.; Wang, X. Water-Mediated Construction And Disassembly Of Self-Assembled Vesicular Supramembranes.
40. Lagalante, A.; Hall, R.; Bruno, T. Kamlet−Taft Solvatochromic Parameters Of The Sub- And Supercritical Fluorinated Ethane Solvents. *The Journal of Physical Chemistry B* 1998, *102* (34), 6601-6604.
41. Lu, J.; Brown, J.; Liotta, C.; Eckert, C. Polarity And Hydrogen-Bonding Of Ambient To Near-Critical Water: Kamlet–Taft Solvent Parameters. *Chemical Communications* 2001, No. 7, 665-666.
42. Geng, S.; Wang, Y.; Wang, L.; Kouyama, T.; Gotoh, T.; Wada, S.; Wang, J. A Light-Responsive Self-Assembly Formed By A Cationic Azobenzene Derivative And SDS As A Drug Delivery System. *Scientific Reports* 2017, *7* (1).
43. Kuiper, J.; Engberts, J. H-Aggregation Of Azobenzene-Substituted Amphiphiles In Vesicular Membranes. *Langmuir* 2004, *20* (4), 1152-1160.
44. Merino, E.; Ribagorda, M. Control Over Molecular Motion Using The Cis–Trans Photoisomerization Of The Azo Group. *Beilstein Journal of Organic Chemistry* 2012, *8*, 1071-1090.
45. Orecchini, A.; Paciaroni, A.; Francesco, A.; Petrillo, C.; Sacchetti, F. Collective Dynamics Of Protein Hydration Water By Brillouin Neutron Spectroscopy. *Journal of the American Chemical Society* 2009, *131* (13), 4664-4669.

7. Appendix

Table S1: The analysis of D_h and PDI of FpC_6Pyrene and FpC_6 MCsome, and the calculation of I_1:I_3 ratio of FpC_6Pyrene MCsome aged at various temperatures.

Temp.*	FpC_6Pyrene MCsome			FpC_6 MCsome		
	D_h / PDI / I_1:I_3 ratio		ΔD_h	D_h / PDI		ΔD_h
	Aging for 24 hours	Aging for 5 days		Aging for 24 hours	Aging for 5 days	
6°C	105 nm / 0.09 / 1.58	99.5 nm / 0.08 / 1.62	- 6 nm	191 nm / 0.05	222 nm / 0.12	31 nm
25°C	108 nm / 0.09 / 1.80	104 nm / 0.09 / 2.08	- 4 nm	221 nm / 0.04	272 nm / 0.02	51 nm
40°C	109 nm / 0.19 / 2.02	119 nm / 0.12 / 2.17	10 nm	N/A	N/A	N/A
50°C	109 nm / 0.14 / 2.05	118 nm / 0.16 / 2.17	9 nm	292 nm / 0.03	precipitate	N/A
70°C	114 nm / 0.11 / 2.08	118 nm / 0.25 / 2.18	4 nm	N/A	N/A	N/A

***The colloids were prepared at 25 °C and aged at different temperatures.**

Table S2: The analysis of D_h and PDI, and the calculation of I_1:I_3 ratio for FpC_6Pyrene MCsome cooled from various temperatures to 6 °C.

Temp*	D_h / PDI / I_1:I_3 ratio			ΔD_h after aging	
	Before cooling**	Cooled to 6 °C (24 hours aging)	Cooled to 6 °C (5 days aging)	24 hours	5 days
40 °C	135 nm / 0.06 / 1.81	127 nm / 0.09 / 1.63	129 nm / 0.06 / 1.60	- 8 nm	- 6 nm
50 °C	137 nm / 0.03 / 2.01	122 nm / 0.05 / 2.06	128 nm / 0.05 / 1.80	- 15 nm	- 9 nm
70 °C	175 nm / 0.15 / 2.08	113 nm / 0.10 / 2.16	122 nm / 0.04 / 2.10	- 62 nm	- 55 nm

*The colloids with a D_h / PDI of 127 nm / 0.09 were prepared at 25 °C and then heated to different temperatures.

**the colloids were aged at the respective temperature for 24 hours

Table S3: The analysis of D_h and PDI, and the calculation of I_1:I_3 ratio of FpC_6Pyrene MCsome cooled from various temperatures to 25 °C.

Temp*	D_h / PDI / I_1:I_3 ratio			ΔD_h after aging	
	Before cooling**	Cooled to 25 °C (24 hours aging)	Cooled to 25 °C (5 days aging)	24 hours	5 days
40 °C	175 nm / 0.11 / 2.00	168 nm / 0.07 / 2.05	177 nm / 0.16 / 1.89	- 7 nm	2 nm
50 °C	181 nm / 0.02 / 2.02	161 nm / 0.11 / 1.92	175 nm / 0.09 / 1.92	- 20 nm	- 6 nm
70 °C	206 nm / 0.08 / 2.06	170 nm / 0.05 / 2.01	171 nm / 0.11 / 1.95	- 36 nm	- 35 nm

*The colloids with a D_h / PDI of 172 nm / 0.12 were prepared at 25 °C and then heated to different temperatures.

**the colloids were aged at the respective temperature for 24 hours